NTNU
Norwegian University of
Science and Technology

Analysis of supermarket CO2 refrigeration cycles equipped with multi-ejectors

Jakub Krzysztof Wiecha

Master of Energy and Environmental Engineering
Submission date: August 2016
Supervisor: Armin Hafner, EPT
Co-supervisor: Andrzej J. Nowak, Silesian University of Technology

Norwegian University of Science and Technology
Department of Energy and Process Engineering

NTNU

Master's Thesis

Analysis of supermarket CO_2 refrigeration cycles equipped with multi-ejectors

Author:

Jakub Wiecha

Department of Energy and Process Engineering

Norwegian University of Science and Technology

Supervisor at Norwegian University of Science and Technology:

Prof. Armin Hafner

Supervisor at Silesian University of Technology:

Prof. Andrzej J. Nowak

Trondheim, July 2016

NTNU

Norwegian University
of Science and Technology

Department of Energy
and Process Engineering

EPT-M-2016-169

MASTER THESIS

for

Student Jakub Wiecha
Spring 2016

Analysis of supermarket CO_2 refrigeration cycles equipped with Multiejectors

Analyse av CO_2 butikk-kjøleanlegg med integrerte multiejektorer

Background and objective

Energy consumptions in supermarkets are among the highest in the building sector. Norwegian supermarkets have a typical energy consumption between 300 to 500 kWh/m²/year, while for office buildings the typical energy consumption is around 100 kWh/m²/year. The main reason for this are the chilling and freezing systems, high ventilation rate and lighting. Energy systems in supermarkets operate after stringent demands and criteria that can be contradictory regarding customers and food stuff in the shop with regard to temperatures and air flows.

Within the scope of MULTIJET project two newly designed R744 supermarket installations has been equipped with Multiejector modules for expansion work recovery and commissioned recently in Trondheim and in Spiazzo Rendena (Italy). A comparative test campaign is ongoing for both supermarkets, based on the measurements of the overall energy consumption in two alternative operation modes: with ejectors (*ejector mode*) and without ejectors (*parallel compression mode*). In order to investigate the annual energy savings due to the Multiejector use, an energy analysis of the entire supermarket energy installation has to be carried out for both locations.

The following tasks are to be considered:

1. Literature review on R744 ejector technology (Introduction to refrigeration cycles, CO_2 R744) as a refrigerant, Overview of R744 refrigeration systems as two-stage cascade refrigeration system, transcritical booster system, transcritical parallel compression system enhanced with ejector technology.
2. Analysis of operating conditions for R744 compressor rack in the two pilot supermarket installations.
3. Establish a plan for dedicated experimental campaigns to be coordinated with the rack-service responsible and shop owners.
4. Initial practical training prior experimental campaigns at the Multiejector test facility at SINTEF/NTNU.
5. Test campaign - collection of experimental data and obtained results.
6. Data processing and analysis of results.
7. Summary and final conclusions.
8. Make a scientific paper with main results from the thesis
9. Make proposal for further work

-- " --

Within 14 days of receiving the written text on the master thesis, the candidate shall submit a research plan for his project to the department.

When the thesis is evaluated, emphasis is put on processing of the results, and that they are presented in tabular and/or graphic form in a clear manner, and that they are analysed carefully.

The thesis should be formulated as a research report with summary both in English and Polish, conclusion, literature references, table of contents etc. During the preparation of the text, the candidate should make an effort to produce a well-structured and easily readable report. In order to ease the evaluation of the thesis, it is important that the cross-references are correct. In the making of the report, strong emphasis should be placed on both a thorough discussion of the results and an orderly presentation.

The candidate is requested to initiate and keep close contact with his/her academic supervisor(s) throughout the working period. The candidate must follow the rules and regulations of NTNU as well as passive directions given by the Department of Energy and Process Engineering.

Risk assessment of the candidate's work shall be carried out according to the department's procedures. The risk assessment must be documented and included as part of the final report. Events related to the candidate's work adversely affecting the health, safety or security, must be documented and included as part of the final report. If the documentation on risk assessment represents a large number of pages, the full version is to be submitted electronically to the supervisor and an excerpt is included in the report.

Pursuant to "Regulations concerning the supplementary provisions to the technology study program/Master of Science" at NTNU §20, the Department reserves the permission to utilize all the results and data for teaching and research purposes as well as in future publications.

The final report is to be submitted digitally in DAIM. An executive summary of the thesis including title, student's name, supervisor's name, year, department name, and NTNU's logo and name, shall be submitted to the department as a separate pdf file. Based on an agreement with the supervisor, the final report and other material and documents may be given to the supervisor in digital format.

☒ Work to be done in lab (Water power lab, Fluids engineering lab, Thermal engineering lab)
☒ Field work

Department of Energy and Process Engineering, March 8th 2016

Prof. Olav Bolland
Department Head

Prof. Armin Hafner
Academic Supervisor
e-mail: armin.hafner@ntnu.no

ACKNOWLEDGMENTS

This master‘s thesis was written within the scope of Multijet project in cooperation with the Department of Energy and Process Engineering at the Norwegian University of Science and Technology (NTNU) in Trondheim (Norway) and the Institute of Thermal Technology at the Silesian University of Technology (SUT) in Gliwice (Poland). I would like to thank my supervisor at the NTNU Prof. Armin Hafner and Prof. Andrzej J. Nowak from the SUT for facilitating my visit in Trondheim.

Trondheim, 25.07.2016

Jakub Wiecha

ABSTRACT

This thesis presents an analysis of operating conditions in a refrigeration system located in supermarket Rema 1000 Prinsensgata, Trondheim (Norway). The main emphasis is put on a problem with oversized gas cooler, which occurs during low ambient temperatures (in winter), and is a root of unstable operation of the whole system. Furthermore, possible solutions to this problem are depicted, among them are: division and cut-down of gas cooler's surface, application of bypassing valve to the gas cooler, triggering fresh air inside supermarket's air-handling-unit (AHU), and utilization of air shutters to the gas cooler. Subsequently, a simulation in a heat exchanger modelling computer program hXSIM (the Heat Exchanger Simulator) of the gas cooler split and increased subcooling is depicted. Lastly, the thesis portrays practical changes which were implemented in the system: exploitation of heat recovery system by snow-melting-unit (street-heating-unit), use of a shut-off valve to decrease the capacity of the gas cooler, implementation of a new controller for the ejectors, reprogramming fans, and also connection of the data acquisition system with energy meters mounted in supermarket's machine room.

STRESZCZENIE

Praca przedstawia analizę waruków pracy w systemie chłodniczym znajdującym się w supermarkecie Rema 1000 w Trondheim (Norwegia). Główny nacisk w pracy został położony na problem napotkany przez przewymiarowaną chłodnicę, który występuje w czasie niskich temperatur otoczenia (zimą) i jest przyczyną niestabilnej pracy system. Ponadto przedstawiono możliwe rozwiązania problemu, wśród których są: podział i zmniejszenie powierzchni chłodnicy, zastosowanie zaworu obejściowego dla chłodnicy, wpuszczenie świeżego powietrza do systemu dostarczającego powietrze do supermarketu oraz zamontowanie kurtyn (zasłon) powietrznych przy chłodnicy. Następnie przeprowadzono symulację w programie służącym do modelowania wymienników cieplnych hXSIM (the Heat Exchanger Simulator), która przedstawia możliwość zastosowania podziału chłodnicy oraz zwiększonego przechłodzenia. Na koniec przedstawiono zmiany jakie w praktyce zostały wprowadzone w systemie: wykorzystanie systemu odzysku ciepła przez układ do topnienia śniegu (ogrzewania ulic), zastosowanie zaworu odcinającego (zamykającego) aby zmniejszyć pojemność cieplną chłodnicy, wdrożenie nowego systemu kontrolującego eżektory, przeprogramowanie wentylatorów oraz podłączenie systemu zbierającego dane z liczników energii elektrycznej zamontowanych w pomieszczeniu chłodniczym supermarketu.

Contents

LIST OF FIGURES

LIST OF TABLES

LIST OF SYMBOLS AND ABBREVIATIONS

Greek Letters

Φ	Mass entrainment ratio	
Π	Pressure Ratio	
η	Efficiency	
ρ	Density	kg/m^3

Roman Letters

v	Specific volume	m^3/kg
h	Specific enthalpy	kJ/kg
$\dot{m}$	Mass flow rate	kg/s
s	Specific entropy	kJ/kg·K
P	Power	kW
p	Pressure	bar
T, t	Temperature	K, °C
$\dot{W}$	Work rate	kW
r	Enthalpy of vaporization	kJ/kg
$\dot{Q}$	Heat rate	kW
$\dot{V}$	Volumetric flow rate	m^3/h
f	Frequency	Hz

Subscripts

is	Isentropic
d	Displacement
rec	Recovered
pot	Potential
comp	Compressor
ej	Ejector
v	Volumetric
diff	Diffuser
evap	Evaporator
in	Inlet

out	Outlet
L	Low-temperature
H	High-temperature
tp	Triple-point
cr	Critical-point

Abbreviations

HFC	Hydrofluorocarbons
CFC	Chlorofluorocarbon
HCFC	Hydrochlorofluorocarbon
ODP	Ozone depletion potential
GWP	Global warming potential
CO_2	Carbon dioxide
R744	Refrigerant signature of carbon dioxide
R717	Refrigerant signature of ammonia
AHU	Air-handling-unit
hXSIM	Heat Exchanger Simulator
GC	Gas cooler
COP	Coefficient of performance
DX	Multiplex direct expansion
HTC	High-temperature circuit
LTC	Low-temperature circuit
MT	Medium-temperature
LT	Low-temperature
SHX	Suction line heat exchanger
rpm	Revolutions per minute
AC	Air conditioning
AUX	Auxiliary
refr	Refrigerant
temp	Temperatur

1. INTRODUCTION

A typical Norwegian supermarket consumes around 300÷500 kWh/m²/year, though 35÷50% of this consumption comes only from refrigeration system. An average supermarket has a refrigeration system based on synthetic refrigerant, which is usually HFC or it former version (i.e. CFC or HCFC), thus posing a threat to the environment. Thanks to the Montreal Protocol on Substances that Deplete the Ozone Layer (1987), which was later followed by several similar protocols, freons are phasing-out, hence a demand for a use of more environmentally friendly refrigerants. As a result, a revival in natural refrigerants occurred in recent years, to displace freons, and also to curb energy consumption in supermarket. Particular properties of CO_2 (denoted by R744) outperform other natural refrigerants (e.g. ammonia), therefore this refrigerant was chosen as an alternative to freons. On this account, a state-of-the-art R744 transcritical parallel vapour compression refrigeration system equipped with multiejector-block with expansion work recovery was invented. Despite many advantages, the system has a very high energy consumption during high ambient temperature, which is a crucial drawback since its application is limited to mild and cold climates. This occurs due to CO_2's low critical temperature (31.05°C), which consequently leads to transcritical mode in the system causing large energy consumption. Nevertheless, in the near future R744 refrigeration systems are expected to work with satisfactory performance worldwide (i.e. in all climate zones). At this point two systems are practically applied, one working in Spiazzo Rendena (Italy), and the second one is implemented in Rema 1000 Prinsensgata in Trondheim (Norway). A test campaign for both systems, carried out within Multijet project in collaboration with NTNU, SUT, SINTEF Energy Research, Enex and Danfoss, is in progress in order to investigate the annual energy savings due to the application of multiejectors.

2. OBJECTIVES

The purpose of this thesis is an analysis of operating conditions in the refrigeration system in Rema 1000 Prinsensgata with an emphasis on the oversized gas cooler in ongoing system, which causes unstable conditions, especially during winter period (low ambient temperature). Moreover, propositions of possible solution to this problem are presented with a simulation in a heat exchanger modelling computer program hXSIM (the Heat Exchanger Simulator). Finally, after few amendments in the system were carried out by the companies working within Multijet project, a comparison of selected parameters was made to investigate the improvement of the system. Nevertheless, due to lingering repairs and continuous problems with the system it was not possible to perform any energy analysis to estimate the overall energy consumption, and to scrutinize the annual energy savings due to the employment of multiejector-block.

3. LITERATURE REVIEW ON R744 EJECTOR TECHNOLOGY

3.1 Introduction to refrigeration cycles

The main purpose of refrigerator is to transmit heat from a cold area (e.g. an ordinary household refrigerator) to a hot (high-temperature) space (like refrigerator's surroundings). This operation (shown in Fig. 3.1) is carried out in cycles by fluids commonly known as refrigerants (Çengel & Boles, 2011).

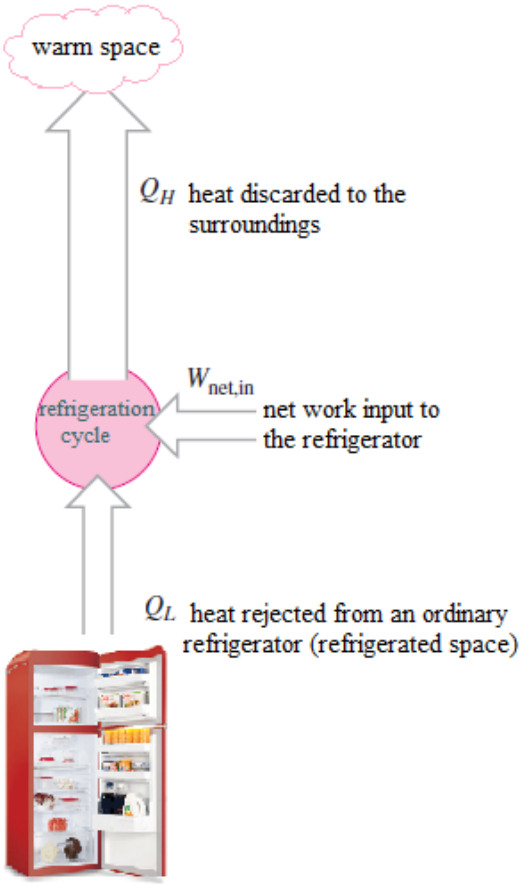

Figure 3.1 Simple schematic of a refrigerator. Adapted and modified from Çengel & Boles (2011)

The most popular and also fundamental refrigeration cycle is the vapour-compression refrigeration cycle. Fig. 3.2 depicts an ideal vapour-compression cycle which is partially based on the reversed Carnot cycle due to severe problems encountered in the latter cycle. On account of difficult compression of vapour-liquid compound in the Carnot cycle, the refrigerant in the ideal cycle enters compressor in a state of saturated vapour. However, in an actual cycle the refrigerant is superheated to guarantee that it is only in one-phase (i.e. vapour). After adiabatic (isentropic) compression (process 1-2 in Fig. 3.2), which is in reality irreversible because of

friction, the refrigerant enters a condenser. During isobaric condensation (process 2-3 in Fig. 3.2) heat is removed to the surroundings, and in the aftermath of that process the refrigerant becomes a saturated liquid. In an actual cycle the refrigerant is additionally subcooled to ensure that it is a liquid which can be subsequently throttled in an expansion valve. Moreover, the lower the temperature (and enthalpy) before the evaporator, the greater amount of heat is absorbed from the refrigerated space. After throttling, which is in the reversed Carnot cycle represented by an adiabatic turbine (state 4s in Fig. 3.2), the refrigerant is vaporized entirely in the evaporator (process 4-1 in Fig. 3.2), and the whole cycle is finished when the refrigerant enters again the compressor. It is worth pointing out that in an actual cycle all components are exposed to inevitable friction, and consequently pressure drop, thus real processes of condensation and evaporation are not isobaric. Therefore, placing all components close to each other is beneficial for the performance of the refrigerator.

The performance of a cycle is described by the coefficient of performance (COP) as (Çengel & Boles, 2011):

$$COP = \frac{\dot{Q}_L}{\dot{W}_{in}} = \frac{T_L}{T_H - T_L} = \frac{1}{\frac{T_H}{T_L} - 1} \tag{1}$$

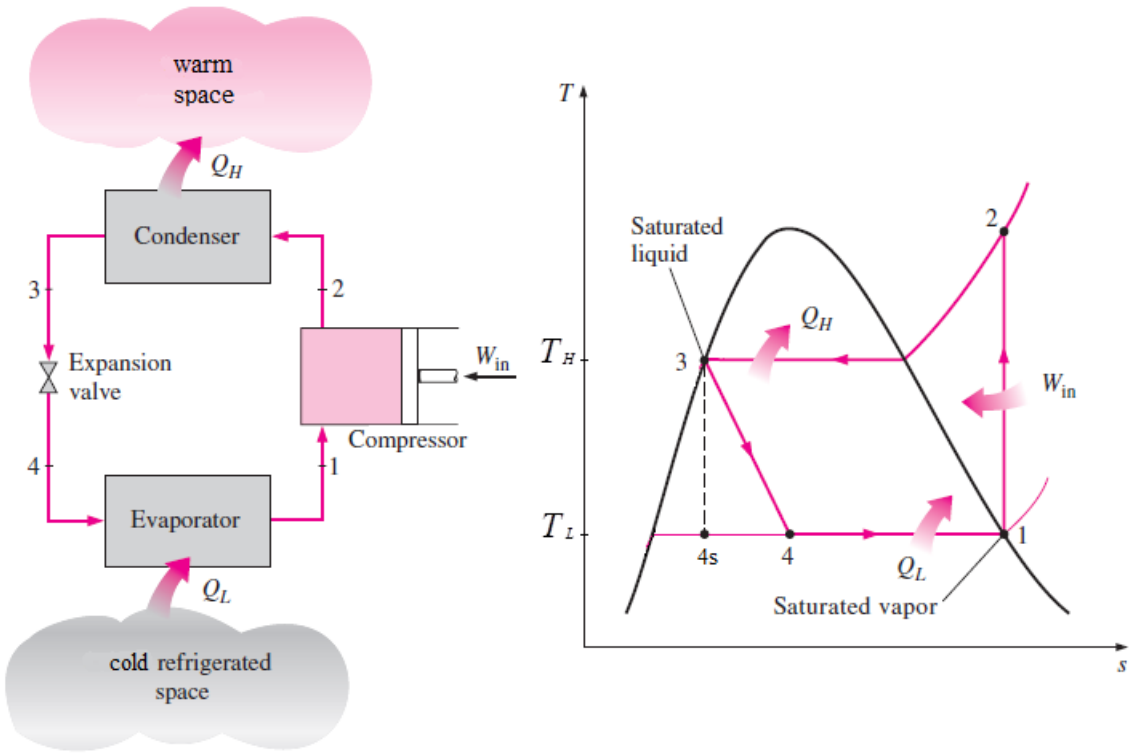

Figure 3.2 The ideal vapour-compression refrigeration cycle. Adapted from Çengel & Boles (2011)

3.2 CO2 (R744) as a refrigerant

According to Freléchox (2009) between 35% to 50% of an average supermarket's energy consumption comes from refrigeration, thus this industry requires the most efficient and environmentally friendly refrigeration systems. Selection of the right refrigerant is a crucial issue while planning a refrigeration system. Commonly used substances as refrigerants are: air (R729), water (R718), ammonia (R717), hydrocarbons (e.g., propane, ethane, ethylene), carbon dioxide (R744), but also synthetic chlorofluorocarbons (CFCs), and hydrochlorofluorocarbons (HCFCs). It should be noted that few of the first refrigerants, such as: sulphur dioxide (R764), methyl chloride (R40) and ethyl chloride (R160), are extremely poisonous. In the aftermath of unfortunate fatalities, the above mentioned substances were prohibited in the 1920s, and substituted by CFCs and HCFCs (like R11, R12, R21, R22, R115, etc.), which are commonly called freons. Nonetheless, in the 1970s it turned out that freons are hazardous, and additionally responsible for ozone depletion, as well as for global warming.

In view of that, few ecological indicators were invented to evaluate usefulness of refrigerants. The most relevant indicators are (Bohdal et al. 2003):

a) ODP (Ozone Depletion Potential) – defines the potential of ozone depletion caused by a substance with reference to freon R11, for which ODP equals 1.
b) GWP (Global Warming Potential) – defines the potential capability of increasing global warming caused by a substance with reference to CO_2, for which GWP equals 1; it is calculated over a particular period of time (usually 100 or 500 years).

Both indicators are shown in Tab. 1 for selected refrigerants. Thanks to the Montreal Protocol on Substances that Deplete the Ozone Layer (1987), which was later followed by several similar protocols, CFCs, HCFCs, halons, methyl bromide, methyl chloroform and carbon tetrachloride were recognized as strikingly harmful, hence the utilization of this refrigerants was significantly cut down, and is nowadays banned (Dinçer & Kanoğlu, 2010). The most dangerous refrigerants are: R11, R12 (substituted by R134a), R113, R114, R502, and also R22 which is considered as a substitute for R12 (Bohdal et al., 2003). Other synthetic substances were invented to substitute CFCs and HCFCs. They are known as HFCs (hydrofluorocarbons), and their advantage is the absence of chlorine which allows them to reach a zero value of ODP rate, but they still have a very high value of GWP index (e.g. for R404a GWP = 3700, Bohdal et al., 2003). For this reasons HFCs are phasing-out and are going to be prohibited in the near future. For fear of the environment, a return to natural refrigerants arises. One of them is ammonia (R717) which is contemporarily used in refrigerators on an industrial scale. R717 has

satisfactory saturation pressure (over temperature of 239.5 K) in the evaporator, which is above atmospheric pressure, therefore any airflow into the refrigerator is avoided. It is essential that the normal boiling point of a refrigerant is below 0°C, for R717 it amounts to -33°C. Secondly, ammonia has very good triple-point parameters, i.e., T_{tp} =195 K, p_{tp} = 6 kPa) . In addition, R717 has high enthalpy of vaporization (e.g. for t =0 °C, r = 1257.6 kJ/kg), thus the mass flow rate is low (Bohdal et al., 2003). Unfortunately ammonia is toxic, flammable, and corrosive, therefore other refrigerants, like CO_2, are tested.

Carbon dioxide was used as a refrigerant for the first time already in 1866 by Thaddeus S. C. Lowe and was implemented in a marine industry. Carbon dioxide was later (in the 1930s) withdrawn with the appearance of freons. A revival took place in the late 1980s, thanks to Prof. Gustav Lorentzen who implied to use R744 in a transcritical cycle (Freléchox, 2009). The main advantages of R744 are: relatively high enthalpy of vaporization (e.g. for t = 0°C, r = 229,48 kJ/kg), low cost, nontoxicity (though high concentration in the air is dangerous), noncorrosivity, nonflammability, and nonexplosivity. Moreover, the ecological properties of CO_2 (shown in Tab. 1) are considered as beneficial in comparison with HFCs, which are defined as "super greenhouse gases". Besides, CO_2 is characterised by unique properties at low temperature: small liquid viscosity, small surface tension, small ratio of liquid to vapour density and high volumetric refrigeration capacity (Bansal, 2012). On the other hand, CO_2 in refrigeration cycles requires high pressures (up to 14 MPa, Chesi et al., 2014) and is characterised by low critical-point properties, namely t_{cr} = 31.05°C and p_{cr} = 7.39 MPa (Dinçer & Kanoğlu, 2010). On this account, the cycle should operate in transcritical mode when condensation temperature is higher than 31.05°C, which occurs in hot climates, or during summer season.

Table 1 Ecological properties of selected refrigerants. Adapted and modified from Grzebielec et al. (2011)

Refrigerant	ODP	GWP	Normal boiling point, °C	Critical temperature, °C	Critical pressure, MPa
R407c	0	1600	-43.8	86	4.63
R717 (ammonia)	0	0	-33	132.4	11.3
R744 (CO_2)	0	1	-57 (triple point at 517 kPa)	31.05	7.39
R12	1	7300	-30	112	4.16
R22	0.05	1700	-41	96.15	4.99

R502	0.33	4300	-45	82.2	4.08
R134a	0	1200	-26.1	101.1	4.06
R290 (propane)	0	3	-42	96.7	4.28
R600a (isobutane)	0	3	-12	135	3.65
R404a	0	3260	-47	72.1	3.73

3.3 Overview of R744 refrigeration systems

Due to specific thermodynamic properties CO_2 is utilized mainly in: indirect, transcritical, or cascade system (Sawalha et al., 2015). The performance of each system rests upon few parameters, like cooling capacity, or ambient conditions. According to Da Silva et al. (2012), greenhouse gas emission from refrigeration systems is considerable, hence a proper study has to be carried out in order to develop a highly-efficient and gas-tight refrigeration system.

A typical refrigeration system applied in supermarket is multiplex direct expansion (DX) system (shown in Fig. 3.3) which usually works with artificial refrigerants, like: R404a, R22, or R507. Moreover, DX system is characterised by high leakage and considerable load of refrigerant. On that account, this system poses a threat to the environment, and other nature friendly refrigeration systems should be developed (Sharma et al., 2014).

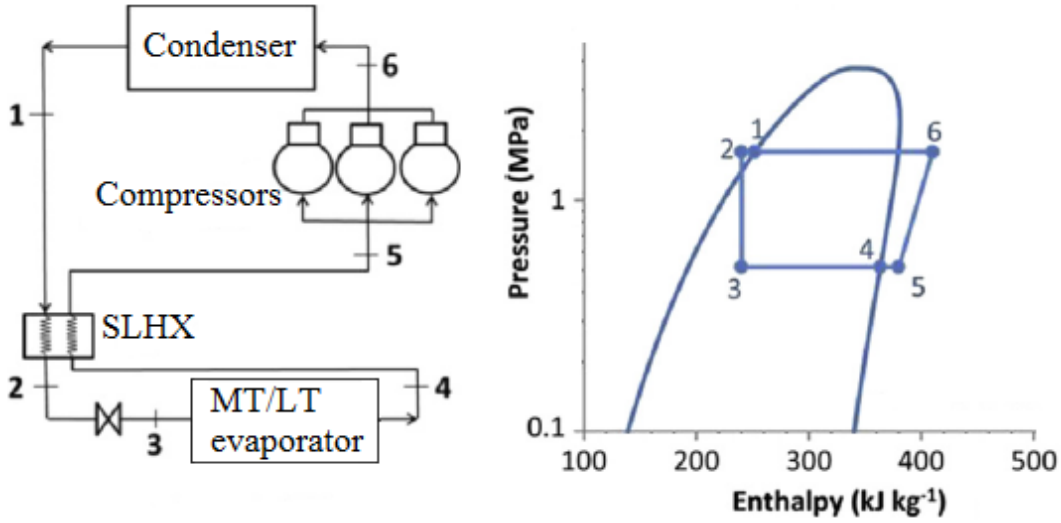

Figure 3.3 Schematic and P-h diagram of the multiplex direct expansion (DX) system. Adapted from Sharma et al. (2014)

1.3.1 Two – stage cascade refrigeration system

A two-stage cascade system includes two independent one-stage cycles which operate with various refrigerants. This system is necessary when one refrigerant is not able to work in a system which demands huge temperature differences between condensation and cold refrigerated space. Due to distinctive thermodynamic properties R744 is applicable in the low-temperature circuit (LTC), whereas in the high-temperature loop (HTC) following refrigerants are usually employed in commercial applications: R404a, R507, propane (R290), propylene (R1270), ethanol, and ammonia (Messineo, 2011). Both circuits (LTC and HTC) are linked to each other by a cascade condenser that operates as an evaporator for the high-temperature loop and as a condenser for the low-temperature loop (shown in Fig. 3.4). According to Messineo (2011) the two-stage cascade system is applicable to supermarket's freezers when the evaporation temperature changes between -30°C and -50°C. In a study conducted by Messineo (2011) the two-stage cascade system with R717 in HTC and R744 in LTC was compared with a HFC (R404a) two-stage refrigeration system. The gist of that analysis is that for typical condensation temperatures (i.e. 35÷40°C), and evaporation temperatures (i.e. -35 ÷ -50°C), both systems achieve similar COPs. Furthermore, for condensation temperatures above 40 degrees Celsius two-stage cascade cycle obtains better performance than the R404a two-stage cycle, but for condensation temperatures lower than 35°C the performance of R404a cycle surpasses the cascade cycle. It is also worth pointing out that for both cycles COP rises by increasing the degree of subcooling. Nonetheless, increasing the degree of superheating has a negligible impact on HFC's cycle, and even decreases the overall system performance of cascade cycle. Finally, when we consider the environmental issues, the R404a contributes greatly to the global warming (GWP = 3700), whereas R744 and R717 are natural refrigerants, thus have much smaller impact on the environment, i.e., GWP = 1, GWP = 0, respectively.

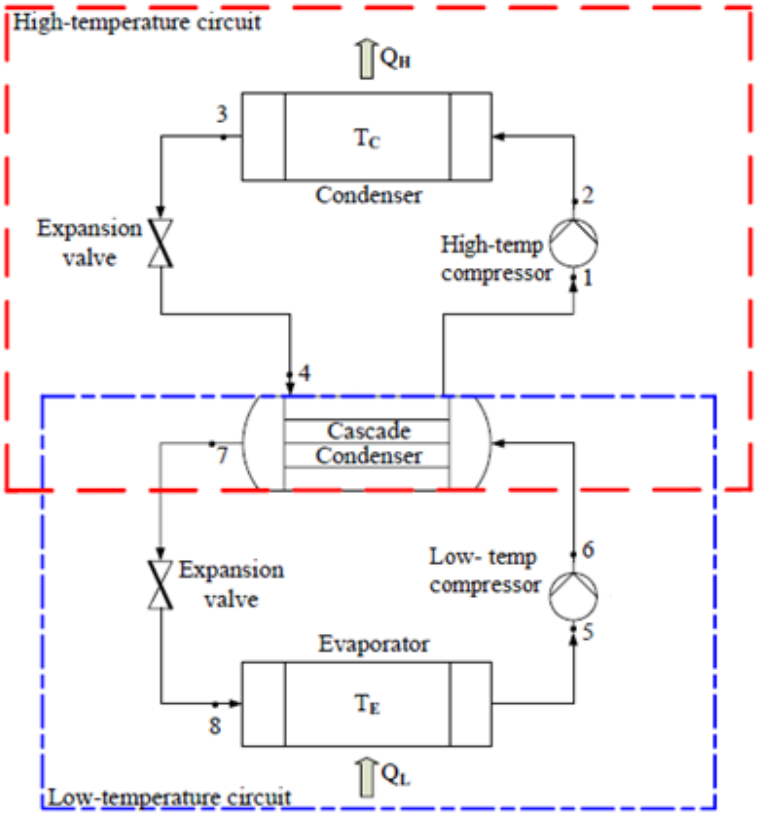

Figure 3.4 Schematic of a two-stage cascade refrigeration system. Adapted and modified from Messineo (2011)

According to other study, carried out by Getu & Bansal (2008), which scrutinised various refrigerants for HTC, the highest COP can be reached with the utilization of ethanol, whereas the lowest COP can be reached with R404a. On the whole, the COP of R717 system is higher than R404a, but lower than ethanol. It should be noted that ethanol is flammable, and requires low saturation pressure in evaporator, as well as in condenser, which is highly below atmospheric, thus leading to an airflow into the system. Another aspect is the mass flow ratio, which is the lowest (among other analysed refrigerants) for ammonia, therefore this refrigerant is considered as the most practical for high-temperature loop of the cascade two-stage cycle.

Different study carried out by Da Silva et al. (2012) compared a cascade system with R744 in LTC, and R404a in HTC with two direct expansion systems, one with R404a, and the second with R22. Conclusions of that study indicate that R404a/R744 system consumes generally less energy (around 13÷24% less than compared systems), is smaller, occupies less space (smaller compressor, evaporator and piping sizes), and demands less refrigerant (that is very cheap). Nevertheless, the cost of the cascade system is around 10÷20% higher than conventional direct expansion systems (Bansal, 2012).

1.3.2 Transcritical booster system

In transcritical booster system CO_2 is used during the whole cycle. The booster system is characterised by one loop (with one refrigerant) which encompasses two temperature levels: medium (MT) and low (LT) level. Furthermore, this system (shown in Fig. 3.5) is fitted with two compressors: high stage, which works in subcritical or transcritical conditions (depending on the ambient temperature), and low stage (booster) compressor, which operates always in subcritical conditions. The system contains four pressure zones: low, medium, intermediate, and high.

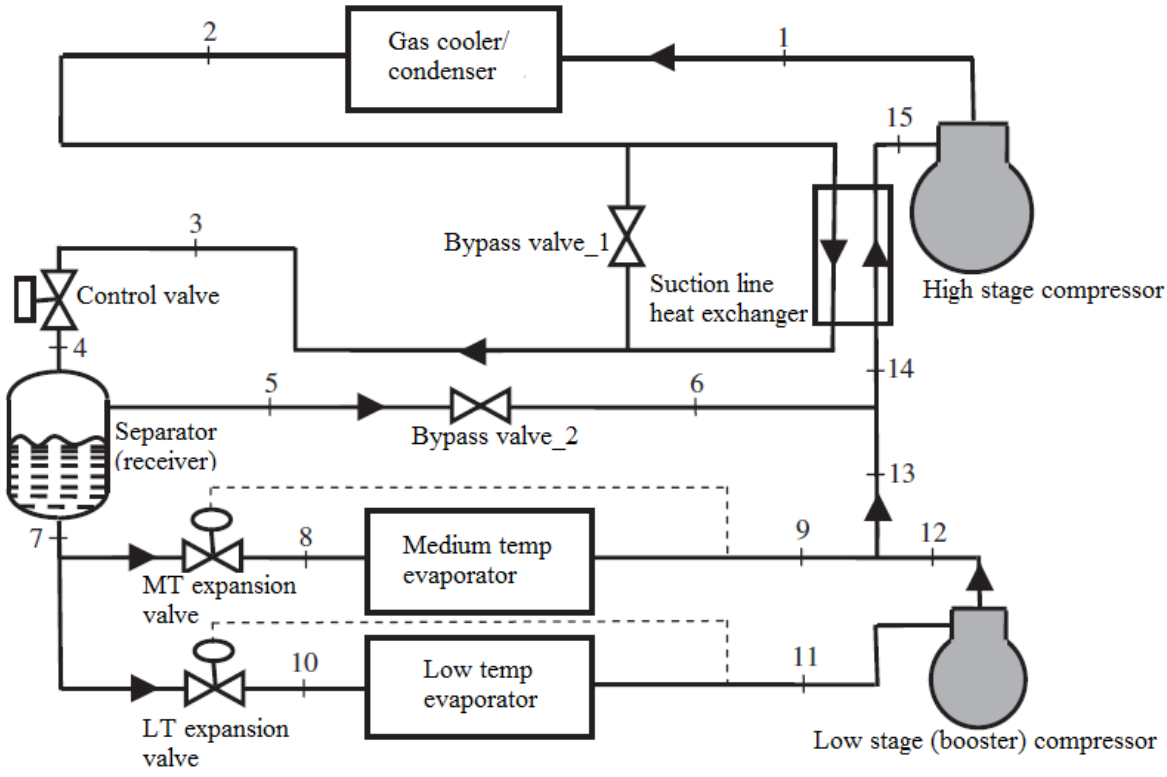

Figure 3.5 Schematic of a transcritical booster system. Adapted and modified from Ge & Tassou (2011)

P-h diagram of transcritical booster system is presented in Fig. 3.6.

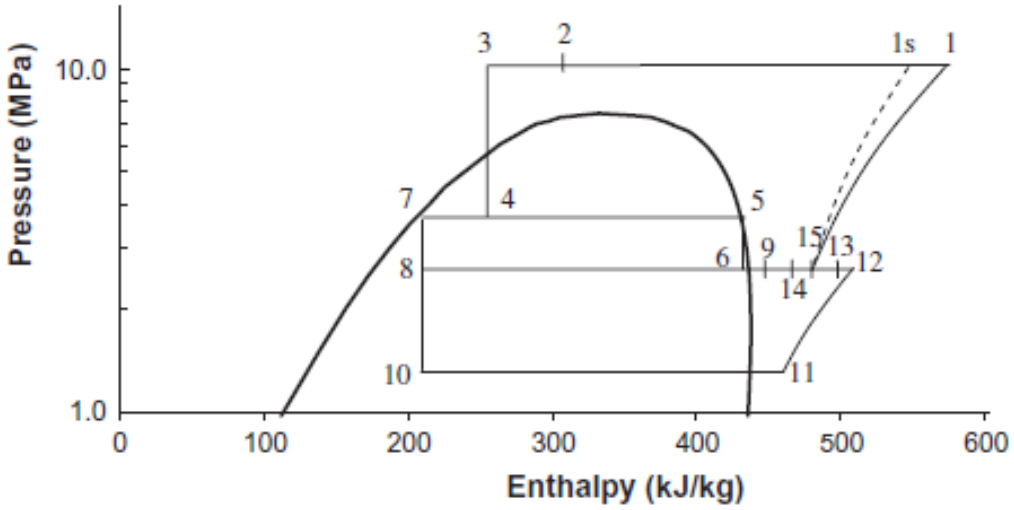

Figure 3.6 Transcritical booster system in P-h layout. Adapted from Ge & Tassou (2011)

The gas cooler/condenser liquefies high-pressure gas (R744) coming from a high-stage compressor. Afterwards, liquid refrigerant enters the suction line heat exchanger (SHX), or flows through bypass valve, providing that the system operates in a subcritical mode. The SHX subcools the refrigerant, which subsequently flows into a liquid receiver (called also separator). On account of expansion, the saturated vapour (called flash gas) separates from liquid R744, and is further throttled by a bypass valve in order to reach MT level. The liquid refrigerant, on the other hand, is throttled via MT- or LT expansion valve, and evaporates in MT- and LT evaporator, respectively. Afterwards, CO_2 in state 11 (in Fig. 3.6) is compressed via low stage (booster) compressor in order to achieve MT level, and mixes with gaseous CO_2 outgoing from MT-evaporator and throttled flash gas (state 6 in Fig. 3.6). Gently superheated refrigerant flows further through the SHX where heat is transferred from liquid (condensed in gas cooler) R744 (state 2 in Fig. 3.6) to the gas phase. Finally, superheated coolant flows through the high-stage compressor, and eventually the whole cycle is finished when the CO_2 enters gas cooler/condenser (Ge & Tassou, 2011). It should be noted that the idea of flash gas enables to whittle down the total mass flow rate in the evaporators, whereas the subcooling in the SHX extends the specific enthalpy difference throughout the evaporators (Bansal, 2012).

According to a study conducted by Girotto et al. (2004), which compared a typical R404a DX system with CO_2 transcritical booster system, in an average medium-sized supermarket (in Treviso, Italy) the COP (for MT- and LT level) of transcritical system is higher than R404a when the average monthly ambient temperature is not higher than 8÷9°C. When the ambient temperature is lower than 15°C system operates in a less energy-consuming subcritical mode.

Therefore, R744 transcritical systems can reach satisfactory performance in rather cold climates of northern and central Europe. It is also worth pointing out that the annual energy consumption is around 10 percent higher for booster system.

1.3.3 Transcritical parallel compression system

Transcritical parallel compression system works similarly to booster system since the former has additional (bypass) compressor for flash gas, and uses two suction liquid heat exchangers (shown in Fig. 3.7). This solution is implemented mainly to decrease the throttling losses (Chesi et al., 2014).

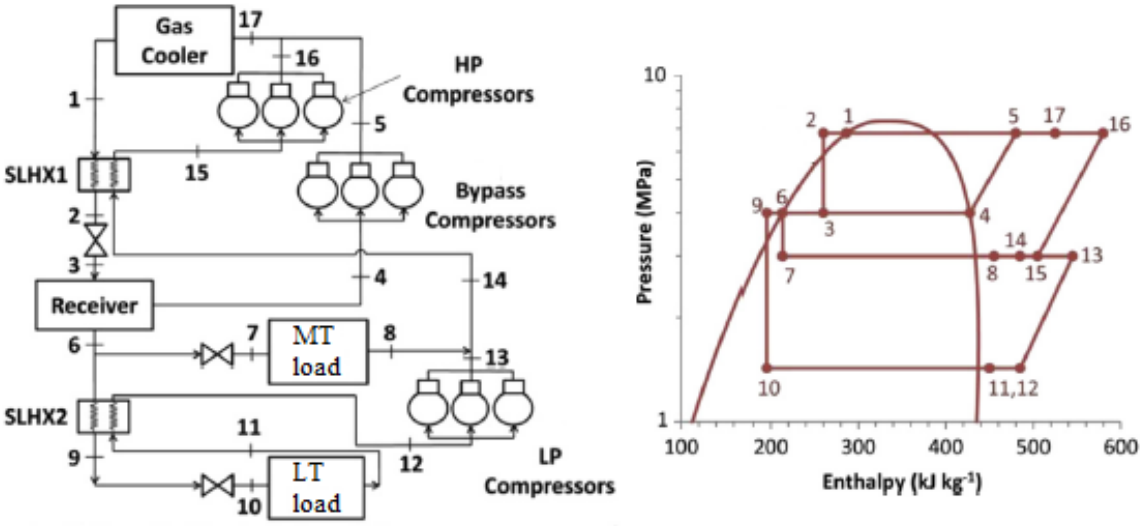

Figure 3.7 Schematic and P-h diagram of transcritical parallel compression system. Adapted from Sharma et al. (2014)

The main amendment in this system allows to make use of flash gas by compressing it by auxiliary (bypass) compressors, thus leading to higher cooling capacity (especially during hot seasons), and eventually higher COP (Bansal, 2012).

Chesi et al. (2014) conducted a study which analysed the influence of various parameters, like: evaporation pressure, compressor discharge pressure, gas cooler outlet temperature, compressor volumetric flow ratio, and receiver separation capacity on the COP. This study indicates that the most unfavourable impact on the COP has low separator efficiency, pressure drops along the lines (especially along the gas cooler), and superheating of evaporated CO_2.

According to an optimization study carried out by Sarkar and Agrawal (2010), which aim was to compare the COP of the transcritical parallel system in three diverse compositions, the

parallel system with economizer (separator) is effective for low-temperature operations. Furthermore, this system reaches (for chosen scope of conditions) much higher COP (47.3% higher over the basic R744 transcritical refrigeration system).

According to a study carried out by Sharma et al. (2014) in eight different climate zones of the USA, the COP of each system depends on the ambient temperature and climate zone. Transcritical booster parallel system reaches the highest efficiency in a rather cold continental and humid climates (i.e. central and northern states of US) when ambient temperature is below 8°C, whereas in hot (southern) climate R404a multiplex DX system is prevalent. However, the average COP over the temperature scope of 0÷40°C for both aforementioned systems is almost identical (Sharma et al., 2014).

Sawalha et al. (2015) carried out field measurements in five Swedish supermarkets to analyse the COP of three types of transcritical refrigeration system. One of them was transcritical booster system with intermediate vessel, which is used after the gas condenser/cooler to remove remnants of gaseous CO_2. This enhancement leads to lower throttling losses, and ultimately to higher COP in compare with basic booster and parallel system. Moreover, higher evaporation temperatures and more efficient compressors are considered as major reasons for the COP improvement. Other different studies confirmed that CO_2 transcritical system has higher or nearly equal COP than traditional HFC system when ambient temperature is lower than 25°C (Sawalha et al. 2015).

3.4. Overview of ejector technology

Ejector technology was implemented due to significant exergy losses (expansion irreversibility) caused by throttling devices (Chesi et al., 2014). Moreover, application of an ejector in the refrigeration cycle decreases compressor's work because of increasing suction pressure, thus prompting higher COP (Sarkar, 2009). In 1858 Henry Giffard came up with an idea of the first ejector, which was precisely a condensing-type injector, and was utilized for pumping water to steam engine boiler's tank. Since that time ejectors have been studied by many researchers, and have a various scope of application, e.g., elimination of non-condensable gases from steam condensers, or emergency pumping of cooling water to nuclear reactor. Besides, they are utilized also in chemical, aviation and aerospace industry, not to mention refrigeration and cooling systems (Elbel, 2011).

1.4.1 Two-phase ejector technology in refrigeration systems

Application of a two-phase ejector in refrigeration cycles (presented in Fig. 3.8) was depicted for the first time in 1931 by Norman H. Gay. This revelation enabled higher cooling capacity due to isentropic processes inside ejector, which consequently yields greater specific enthalpy difference along the evaporator compared to typical (isenthalpic) expansion valve. Furthermore, as it was already mentioned, two-phase ejector contributes to the reduction of compressor work.

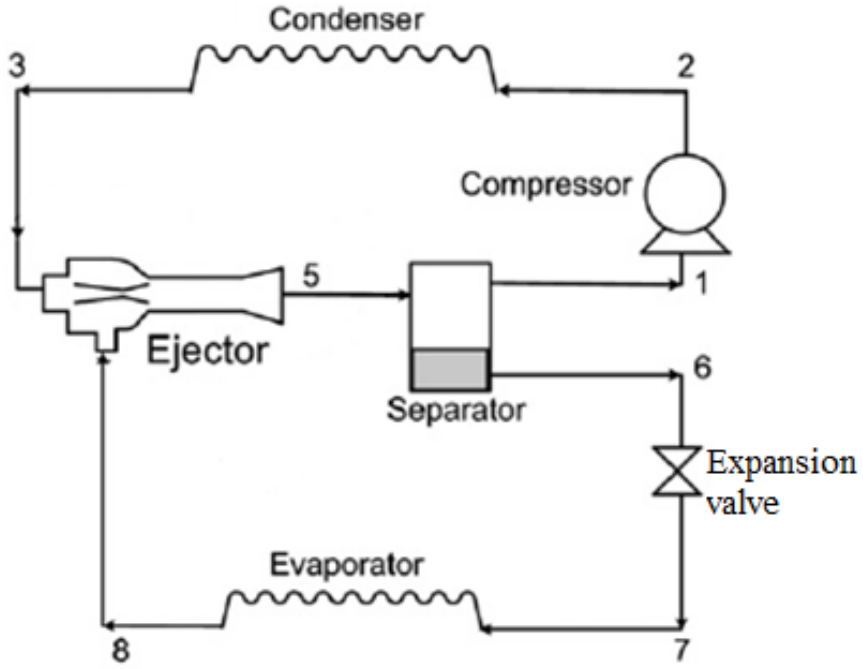

Figure 3.8 Schematic of R744 vapour compression refrigeration cycle with a two-phase ejector. Adapted from Sumeru et al. (2012)

Comparison between a cycle with typical expansion device and two-phase ejector is shown in Fig. 3.9. Higher suction pressure (state 1 for the ejector, state 8 for typical expansion device in Fig. 3.9) allows to diminish compression ratio, and this eventually leads to higher compressor efficiency (Elbel, 2011).

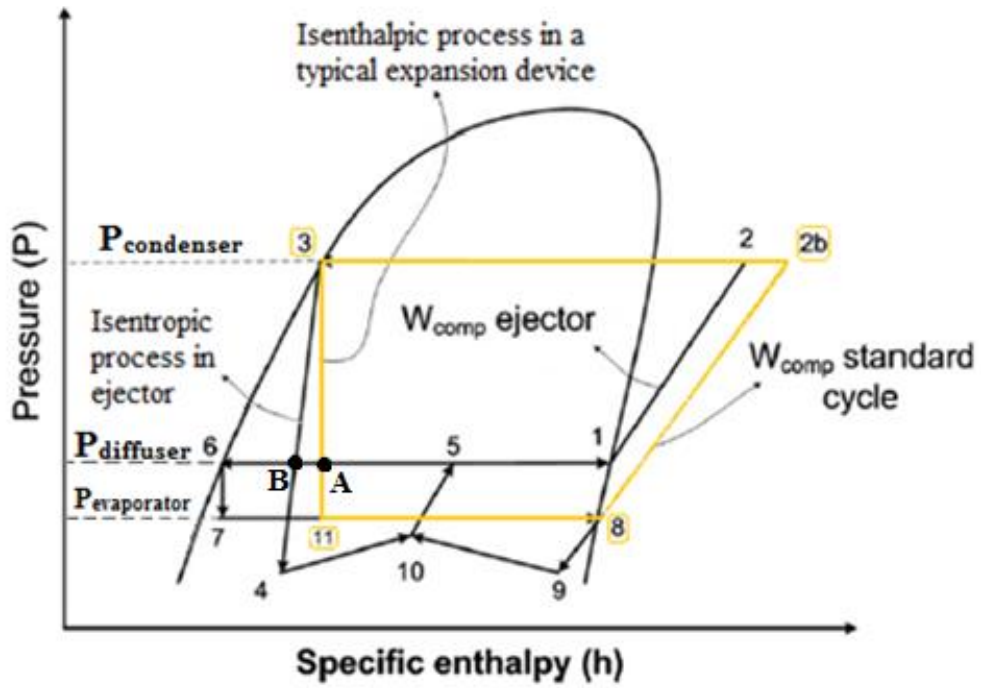

Figure 3.9 P-h diagram of R744 vapour compression refrigeration cycle with a two-phase ejector and comparison with standard cycle. Adapted and modified from Sumeru et al. (2012)

Two types of ejector can be distinguished, namely, a constant-area mixing ejector and a constant-pressure mixing ejector. Commonly utilized in different refrigeration applications is the constant-pressure mixing ejector, however, Yapici & Ersoy (2005) proved that for the same operating temperature the constant-area mixing ejector achieves higher COP than the constant-pressure mixing ejector. For that reason researchers employ ordinarily the constant-area mixing ejector for the numerical and experimental studies (Sumeru et al., 2012).

In the two-phase ejector driving flow is liquid, whereas driven flow is vapour. The constant-area mixing ejector (shown in Fig. 3.10) is comprised of three sections: nozzle (suction section), constant-area mixing section, and diffuser. The primary (motive) high pressure stream from condenser/gas cooler enters the converging-diverging (motive) nozzle, which allows to accelerate (increase kinetic energy) its flow to supersonic level for transcritical parameters. The motive flow expands isentropically (point 3 to 4 in Fig. 3.10) to the mixing pressure. The narrowest element in motive nozzle is called throat. Meanwhile, the secondary low pressure stream is captured (entrained) by the motive stream (point 8 to 9 in Fig. 3.10). Both flows mix at the inlet of constant-area mixing section, thus creating an intricate phenomena that involves momentum transfer. Afterwards, the two-phase mixture enters the diffuser, where its kinetic energy transforms into pressure energy, causing isentropic compression (point 10 to 5 in Fig. 3.10). Finally the mixture leaves ejector and enters the separator, which passes the vapour

fraction to the compressor-condenser /gas cooler-ejector-separator circuit (points 1-2-3-5-1 in Fig. 3.8 or points 1-2-3-4-10-5-1 in Fig. 3.9), and the liquid fraction to the expansion valve-evaporator-ejector-separator circuit (points 6-7-8-5-6 in Fig. 3.8 or points point 6-7-8-9-10-5-6 in Fig. 3.9) (Sumeru et al., 2012). Besides, it should be pointed out that ejector is able to work (entrain) as long as the pressure at the inlet of the mixing chamber is lower than (low-pressure) secondary stream leaving the evaporator (Elbel, 2011).

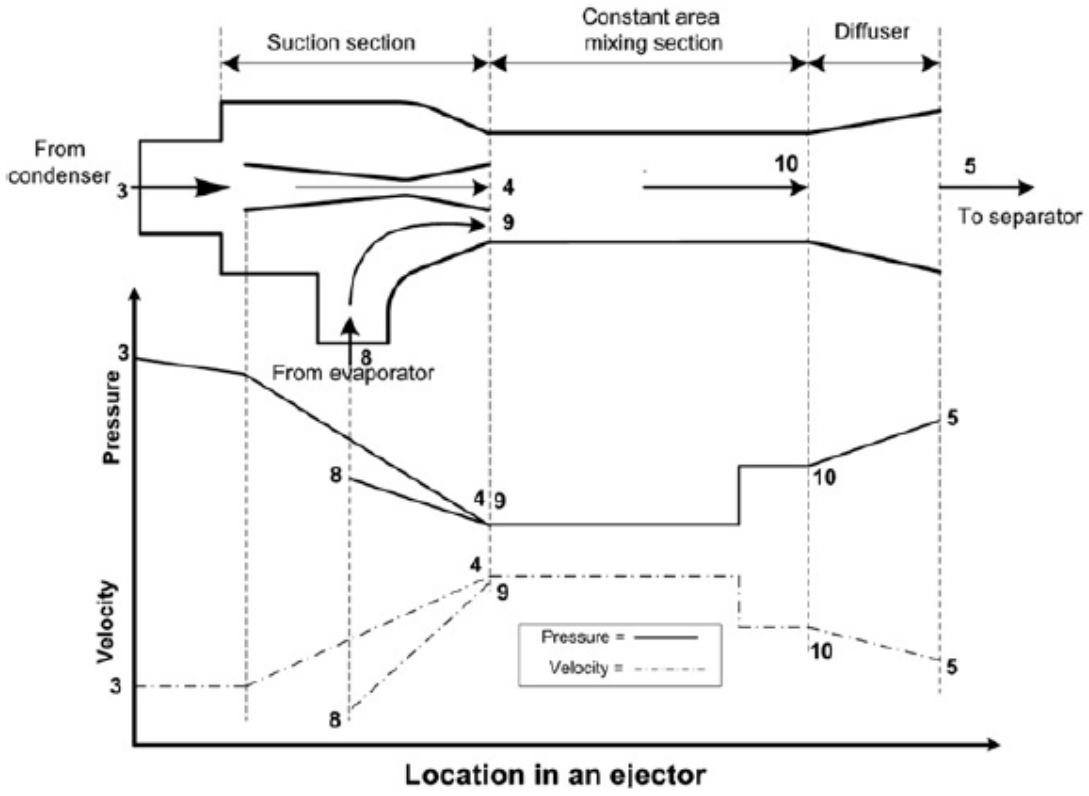

Figure 3.10 Pressure and velocity profile inside a two-phase ejector. Adapted from Sumeru et al. (2012)

The ejector performance can be evaluated by: mass entrainment ratio (Eq. 2), suction pressure ratio (lifting ratio) (Eq. 3), or ejector efficiency (Eq. 4) invented by Elbel & Hrnjak (2008), which shows a ratio of recovered expansion work rate ($\dot{W}_{rec}$) in relation with work recovery potential rate ($\dot{W}_{pot,rec}$). Points A and B are referenced to Figure 1.9 (Elbel, 2011).

$$\phi = \frac{\dot{m}_{suction}}{\dot{m}_{motive}} \tag{2}$$

$$\Pi = \frac{P_{diff,out}}{P_{evap,out}} \tag{3}$$

$$\eta_{ejec} = \frac{(h_1 - h_8)}{(h_A - h_B)} \cdot \frac{\dot{m}_{suction}}{\dot{m}_{motive}} = \phi \cdot \frac{(h_1 - h_8)}{(h_A - h_B)} = \frac{\dot{W}_{rec}}{\dot{W}_{pot,rec}} \quad (4)$$

High suction pressure ratio contributes to a decline in compression ratio (of the compressor), whereas large mass entrainment ratio provides lower compressor flow rates for particular cooling capacity. On the other hand, Eq. 4 (ejector efficiency) describes recovered work (difference between points 1 and 8 in Fig. 3.9) due to isentropic expansion and potential recovery of work (difference between points B and A in Fig. 3.9) thanks to isentropic expansion (Elbel, 2011). Nonetheless, the entrainment ratio cannot be raised as high as possible since it would cut down the flow of motive stream (Sumeru et al., 2012).

First numerical study of the two-phase ejector was carried out by Kornhauser (1990). In this study a one-dimensional model was implemented to compare COP of vapour compression cycle with standard expansion valve and two-phase ejector for selected refrigerants. The results proved that the COP of ejector expansion cycle is generally higher than standard cycle. The highest increase in COP achieved: R-502 (the COP improved 1.3 times), R-114 (the COP enhanced 1.24 times), and for R717 the COP went up 1.12 times. Kornhauser's study caused intensive research in search for improvement of ejector technology for different refrigerants, including R744.

Another study, carried out by Menegay & Kornhauser (1996), used patented in 1994 bubbles breaker device to increase velocity of stream at the motive nozzle. The analysis confirmed that the COP of ejector expansion refrigeration system with R12 and bubbly flow tube improved (in comparison to standard vapour compression cycle) from 3.2% to 3.8%, whereas without bubbly flow tube in the range of 2.3÷3.1%.

Li & Groll (2005) conducted a thermodynamic analysis of the ejector expansion transcritical R744 cycle with a constant pressure-mixing model. The study corroborated that the COP of transcritical cycle with the ejector outperforms significantly standard cycle, in case of typical air conditioning applications the improvement amounts to more than 16%.

Deng et al. (2007) executed a numerical (exergy and energy) analysis of the transcritical R744 ejector expansion cycle to compare its COP with an internal heat exchanger cycle and a standard vapour compression cycle. The results showed that the COP of ejector expansion cycle improved by 18.6% over internal heat exchanger cycle, and 22% over conventional cycle. The exergy analysis pointed out that exergy loss from expansion in the typical cycle constitutes

34.29% of the entire exergy loss, while in the ejector expansion cycle it was only 29.7% of the total exergy loss.

Elbel & Hrnjak (2008) implemented a prototype ejector with a variable motive nozzle area in which the high-side pressure was changing for different settings of needle. The experimental study compared the COP of standard refrigeration cycle with the COP of transcritical R744 ejector expansion cycle with three different diffuser angles. The results showed that the highest improvement over conventional cycle (by 7% for the COP and 8% for the cooling capacity) was reached for the smallest diffuser angle (of 5°), and for the smallest area of motive nozzle's throat, which was decreasing with the increase in high-side pressure. It is also worth mentioning that when the high-side pressure increases, the total efficiency of the ejector de facto diminishes.

Chaiwongsa & Wongwises (2007) scrutinised the effect of throat diameter of the two-phase ejector expansion cycle on the COP. The results showed that the highest COP is reached for throat's diameter tantamount to 0.8 mm. This causes a low motive flow rate, although cooling capacity and vaporized mass flow rate of the cycle remain high.

Elbel (2011) investigated the impact of the diffuser angle and changes in the mixing section length on the ejector efficiency and on the COP of CO_2 transcritical system. For diffuser, angles between 3° and 15° were analysed, while for the mixing section (diameter was constant and equal 2.8 mm) four different lengths (7.5 mm, 32.5 mm, 57.5 mm and 82.5 mm) were scrutinised. The results indicated that the shortest length (7.5 mm) yields the highest ejector efficiencies (of up to 15%), whereas for the diffuser angle the best ejector efficiencies were registered for 5°. The results proved the COP improvement with the same results as the study conducted by Elbel & Hrnjak (2008).

According to Sumeru et al. (2012) a two-phase ejector used as an expansion device improves the COP of the vapour compression refrigeration cycle by 20%, but the improvement recorded during practical experiments was never higher than 10%. Besides, the study indicates areas that could have a crucial impact on the COP of the cycle, and thus should be investigated in the future, such as: diffuser, throat of the motive nozzle, suction chamber, and constant area section. In conclusion, the two-phase ejector requires further development to substitute traditional expansion device. and to achieve satisfactory performance in refrigeration systems.

4. ANALYSIS OF THE REFRIGERATION SYSTEM IN REMA 1000 PRINSENSGATA

The refrigeration system in Rema 1000 Prinsensgata is a R744 transcritical parallel compression system equipped with multi-ejector block (shown in Fig. 4.1).

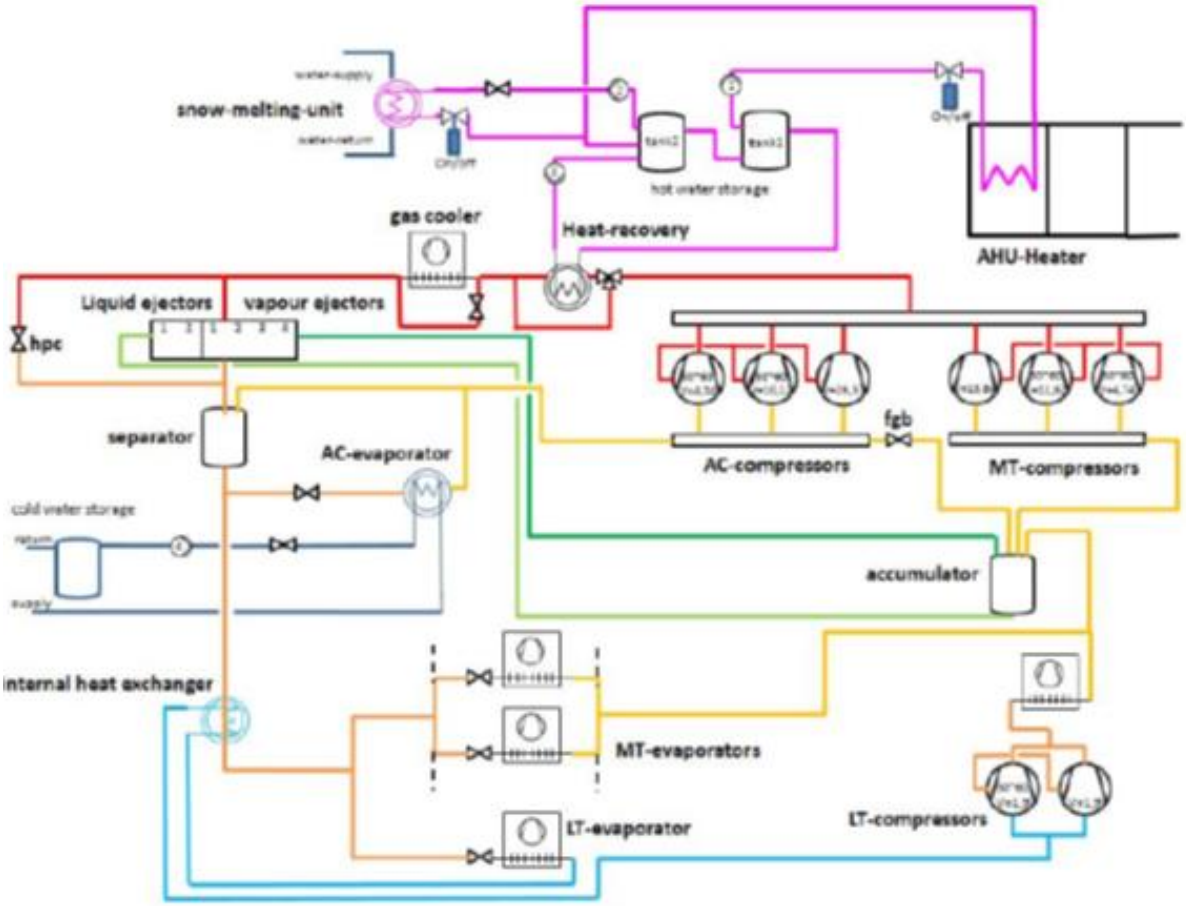

Figure 4.1 Simplified scheme of the refrigeration system in Trondheim. Adapted from Herdlitschka (2016)

The system is located in one building with offices. It produces cold for chilling cabinets in the supermarket and ice-water for air conditioning in the whole building. Moreover, surplus of the hot CO_2 in the high-pressure section is utilized in the air handling unit (AHU) to warm up air incoming to the supermarket and also by the snow-melting-unit after snowfalls. Gas cooler (presented in Fig. 4.2 and Fig. 4.3) has an internal volume of 99.7 litres and a calculated (designed) capacity of 368 kW (at 20 °C ambient temperature). The gas cooler is supported by 6 fans with total nominal power of 1260 W. The rpm of the fans is determined by the refrigerant outlet temperature and ambient temperature. After the gas cooler, liquid CO_2 expands in the

multi-ejector block, which collaborates with a high pressure electronic valve (hpc). The suction side of the ejectors is connected with the accumulator (liquid receiver) by either vapour (for vapour ejectors) or liquid (for liquid ejectors). As a consequence, a mixture of gas and liquid reaches liquid separator, where the gaseous phase is transported by a flash-gas throttling valve to the accumulator, or is taken by the AC-compressors in order to keep up steady pressure conditions in the separator. Meanwhile, the liquid refrigerant proceeds to LT- and MT-evaporators being on the way utilized by AC-evaporator in the event of air conditioning demand, and finally cools down in the internal heat exchanger. LT-evaporator charges LT-compressors (set point at 13 bar, -33°C) with slightly superheated vapour, which is compressed to a medium (MT) pressure level, than precooled before it mixes with vapour produced by MT-evaporators, and finally enters the accumulator. The accumulator distributes refrigerant to the multi-ejector block and to the MT-compressors, which work with a suction pressure of 30.5 bar (i.e. saturation temperature equal to -5°C). In case of increasing load of the system, AC-compressors begin to work (set point at 38.7 bar, 4°C). This situation occurs when ¼ of the flash-gas bypassing valve is open for more than 1 minute and at the same time gas cooler outlet temperature is not lower than 15°C. Heat recovery system works during the winter to melt down snow or heat up fresh air coming through the AHU to the supermarket.

Figure 4.2 Gas cooler on the roof of Rema 1000 Prinsensgata, rear view

Figure 4.3 Gas cooler on the roof of Rema 1000 Prinsensgata, side view

Closer front view of the gas cooler, marked with headers and refrigerant loops (blue arrow denotes refrigerant's flow), is presented in Fig. 4.4.

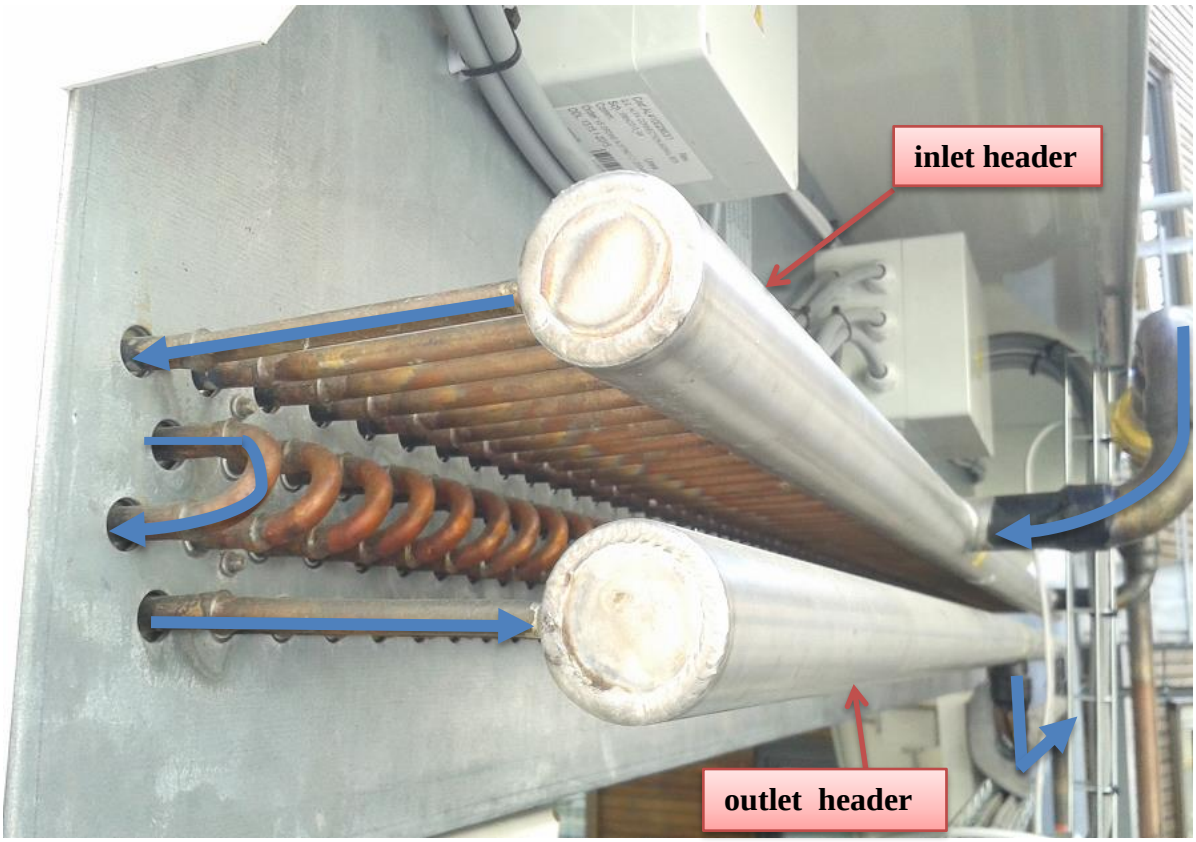

Figure 4.4 Gas cooler on the roof of Rema 1000 Prinsensgata, close-up view

The rack of compressors is comprised of (Herdlitschka, 2016):

1) MT- compressors:

- Compressor 1: Dorin CD 750H, displacement: 4.74 m³/h at 50 Hz, frequency controlled (30 ÷ 60 Hz)
- Compressor 2: Dorin CD 1400M, displacement: 11.62 m³/h at 50 Hz, frequency controlled (30 ÷ 60 Hz)
- Compressor 3: Dorin CD 2000M, displacement: 13.84 m³/h at 50 Hz, on/off controlled

The total capacity of the MT-compressors varies between 8.089÷97.591 kW.

2) AC-compressors (parallel compressors):

- Compressor 1: Dorin CD 700H, displacement: 4.34 m³/h at 50 Hz, frequency controlled (30 ÷ 60 Hz)
- Compressor 2: Dorin CD 1500H, displacement: 10.12 m³/h at 50 Hz, frequency controlled (30 ÷ 60 Hz)
- Compressor 3: Dorin CD 4000H, displacement: 26.57 m³/h at 50 Hz, on/off controlled

The total capacity of the AC-compressors changes from 9.144÷157.596 kW.

3) LT-compressors:

Two Dorin CDS 101B compressors, displacement: 1.9 m^3/h at 50 Hz. Just one compressor is frequency controlled (30 ÷ 60 Hz) and the second one is switched on or off. This gives the total capacity diverging from 2.837 kW to 10.402 kW.

4.1 Problems with the gas cooler during winter operation

As a result of a large size of the gas cooler (368 kW) at summer high load conditions, the system encounters considerable problems when running in winter (low ambient temperature) with low load (10÷20% MT load). The problem occurs when the gas cooler (GC) outlet temperature rises because of increasing flow of CO_2 entering the GC, which originally aims to prevent low outlet temperature (and pressure). This then induces a rise in the requested GC outlet pressure, which results in closing ejectors and stopping the refrigerant flow in order to obtain this pressure by charging up the gas cooler. This situation takes place approximately every 7÷8 minutes. Afterwards, the temperature sensor, which is located behind the GC outlet, sends false signal to the fans informing of an excessive outlet temperature, but there is no refrigerant flow at that moment. Consequently, this action triggers blowers to diminish the refrigerant temperature even if it is already very low. Thereafter, the GC outlet pressure finally reaches requested pressure as long the ejectors stay closed. After that, ejectors open to maintain the GC outlet pressure. Firstly, the very cold refrigerant leaves the GC, which is followed by warmer CO_2. Finally, the refrigerant flow increases and the requested pressure rises. Thus, the GC outlet temperature increases and the whole vicious cycle (shown in Fig. 4.5) begins again.

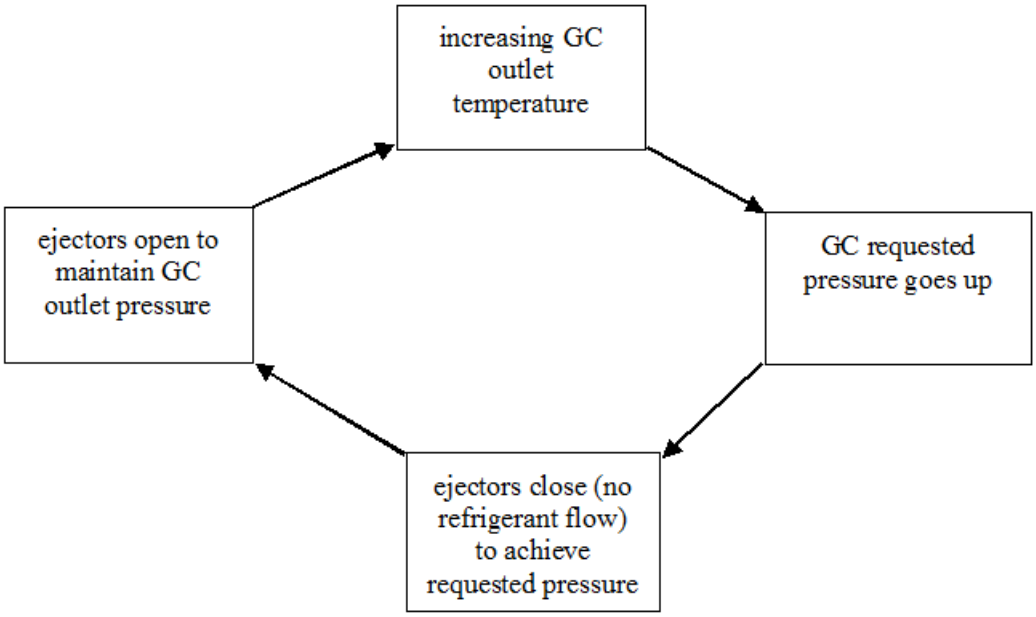

Figure 4.5 Simplified schema of gas cooler's incorrect work with low load

4.2 Possible solutions for the gas cooler

In order to avoid problems discussed in section 4.1 following solution should be taken into consideration:

1) The gas cooler could be divided into two parts, whereas the first part is 1/3 of the total length (with two fans) and the second part comprises 2/3 of the total length (with one fan). Just 50 percent of the GC capacity could be used (the rest can be shut off) when the ambient temperature is low since it is enough to support chilling cabinets in supermarket and air conditioning for the whole building. The former part should provide liquid CO_2 at the outlet while the latter part should subcool further liquid refrigerant by at least 5 K. Eventually, the final temperature (after the gas cooler) cannot be lower than 5°C owing to the fact that lower temperatures are not appropriate for liquid separator's pressure level. The separator aims to provide saturated liquid to the evaporators and flash-gas to either AC-compressors or accumulator. Fig. 4.6 presents a p-h diagram with border line (marked in yellow) denoting boundary acceptable outlet parameters, and two exemplary cycles, where the process marked in brown presents unfavourable conditions because of very low gas cooler outlet temperature. In this case, low pressure in the separator (below 40 bar) inhibits refrigerant supply to the cabinets, thus very low pressure (and temperature) at the suction of MT-compressors (set point at -5°C) causes the compressors to shut off and eventually the whole system collapses. To prevent this situation gas cooler outlet temperature should not be lower than around 5°C though this temperature always fluctuates due to the influence of wind.

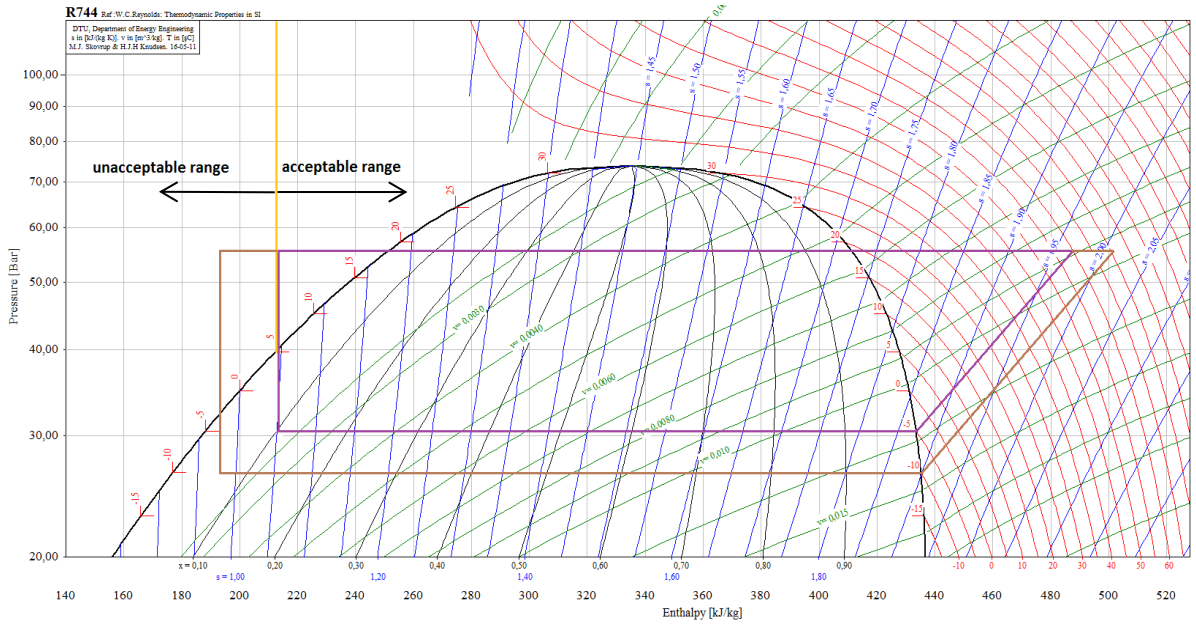

Figure 4.6 Simplified p-h diagram of R744 refrigeration cycle with acceptable gas cooler outlet parameters (in violet) and exemplary unacceptable parameters (in brown)

In this solution a bypassing valve could be installed after the first part of the GC if sufficient subcooling is provided. The second part of the gas cooler would not have to be utilized, which could lead to certain energy savings. This solution could be implemented in future projects since rebuilding the gas cooler working in the current unit in Rema Prinsensgata is impossible. A sketch of this concept is shown in Fig. 4.7.

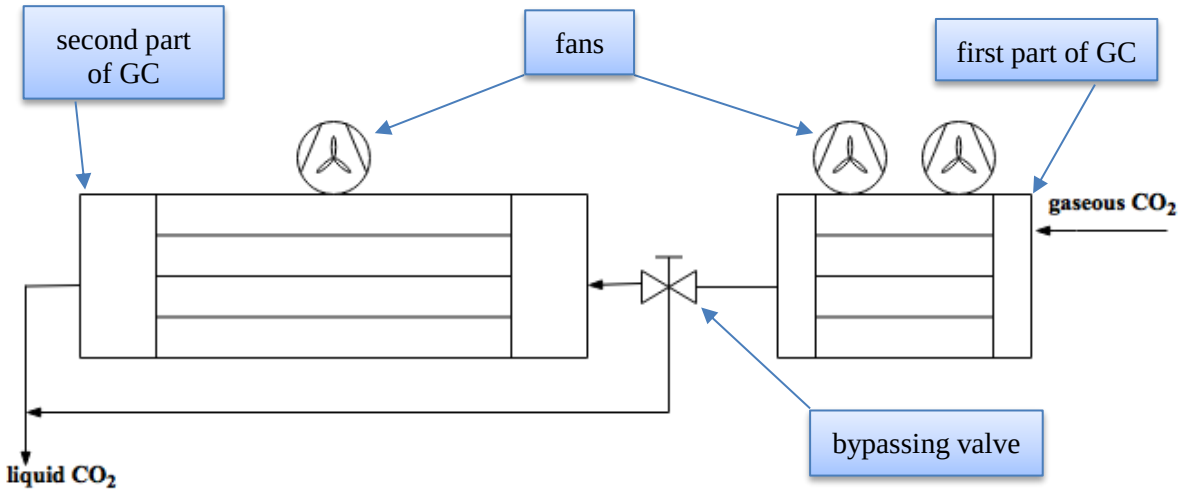

Figure 4.7 Gas cooler divided into two parts with bypassing valve

2) The gas cooler could comprise even of one element containing two (aforesaid) parts. In this case, the second part would be cooled by a fan running very slowly, creating conditions close to natural convection. Nonetheless, in this instance air shutters should be installed in order to constrain (cold) ambient air entering the gas cooler when fans come to a halt, thus avoiding a risk of low CO_2 outlet temperature. This solution originates from automotive industry (shown in Fig. 4.8). This idea might be used perhaps in the future, but is not a quick fix for the existing system in Prinsensgata.

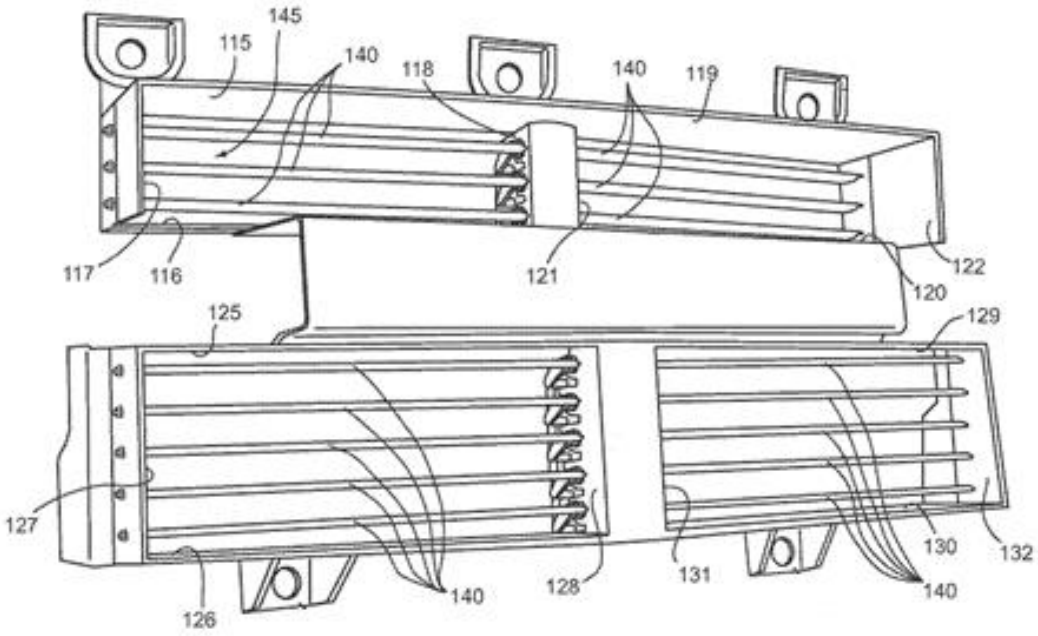

Figure 4.8 Active grill shutter vane design and vehicle system. Adapted from Pastrick et al. (2013)

A sketch of this concept applied in a gas cooler is presented in Fig. 4.9.

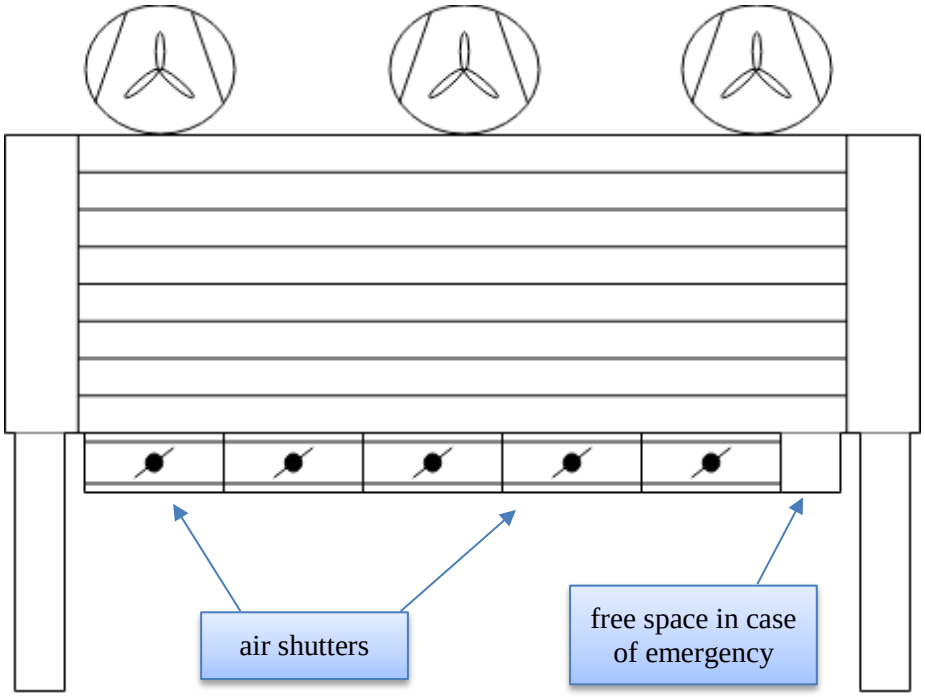

Figure 4.9 Air shutters mounted on the gas cooler

3) There are few possible solution that could be implemented in the ongoing system in Prinsensgata. One of the option is to intensify the utilization of heat recovery system. The heat recovery system (street heating) could work even for the whole year, thus it would be possible to bypass the gas cooler, in order to approach outlet set parameters. The heat might be used not only to heat up streets during winter, but also to dry up streets after rainfalls in other seasons. In addition, the inflow of fresh air to the grocery store could be more frequent, owing to the fact that rejected heat might heat up fresh air more often than in currently working system. In the present system supermarket's ventilation system operates just in recirculation mode, which means that fresh ambient air enters only if the content of CO_2 in the market's air reaches a set-point. To change that, snow-melting-unit's circulation pump should be perpetually turned on. On the question of AHU-heater, in order to heat up ambient air, a temperature sensor should send a signal to the ventilation system to let in fresh air to the supermarket when sufficient temperature has been reached inside the storage tanks. In this way problems with a low gas cooler outlet temperature could be prevented during cold days. Another option is a shut-off valve, which aims to decrease gas cooler's capacity when the ambient temperature is low.

5. SIMULATION OF POSSIBLE SOLUTIONS FOR THE GAS COOLER

5.1 Objectives of simulation

The main purpose of this analysis is to obtain the GC outlet temperature in an acceptable range for liquid separator's pressure level in view of the gas cooler split-up into two parts, and increased subcooling with relatively fixed GC outlet pressure (around 55 bar), which should lead to more stabilised operation of the whole system and eventually an increase in the COP. Investigation of the effect of splitting gas cooler into two parts was carried out in a heat exchanger modelling computer program hXSIM (the Heat Exchanger Simulator) v5.04-2007. This program was established at SINTEF Energy Research by G. Skaugen (2000 & 2002). In this program the user is able to specify the type of heat exchanger (e.g. gas cooler, air cooler, condenser, evaporator, free cooler), as well as many tube and fin variants. hXSIM computes the overall heat exchanger performance by determining the heat balance between the air side and refrigerant side. An example of simulation's panel is presented in Fig. 5.1.

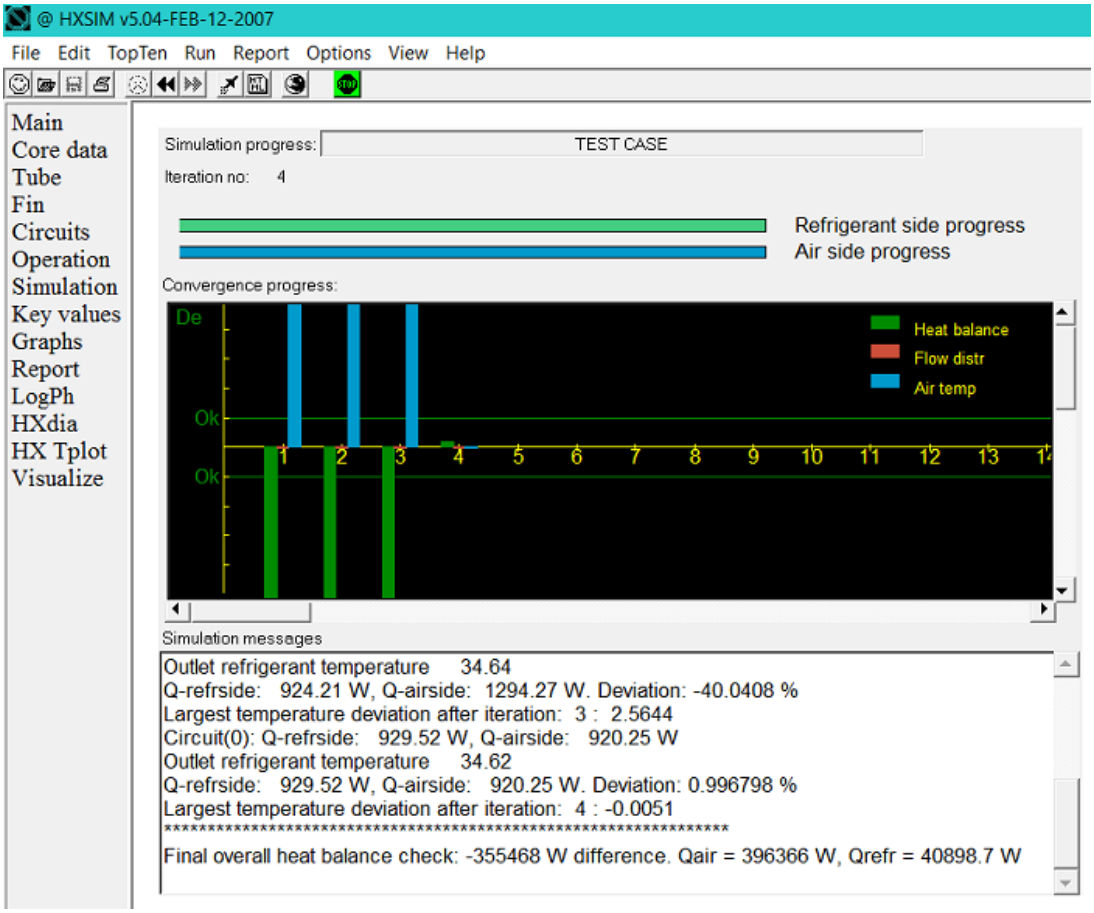

Figure 5.1 Simulation's panel in hXSIM

The overall heat exchanger performance is computed by calculating local heat transfer and pressure drop gradients, and subsequently integrating them along every refrigerant loop (Hafner, 2003). Moreover, the program draws temperature profiles of streams passing through the heat exchanger. Exemplary profiles are shown in Fig. 5.2.

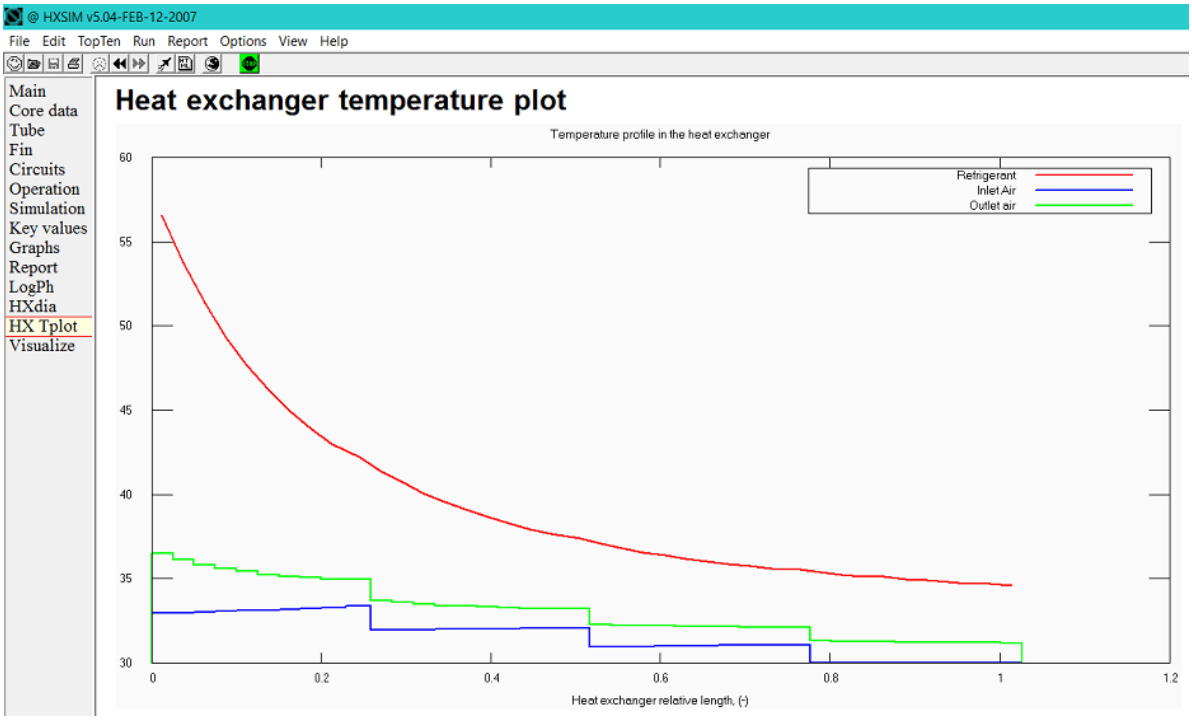

Figure 5.2 Temperature profiles of streams passing through the heat exchanger in hXSIM

Additionally, hXSIM presents after completed simulation a simple sketch (visualisation) of projected heat exchanger (shown in Fig 5.3).

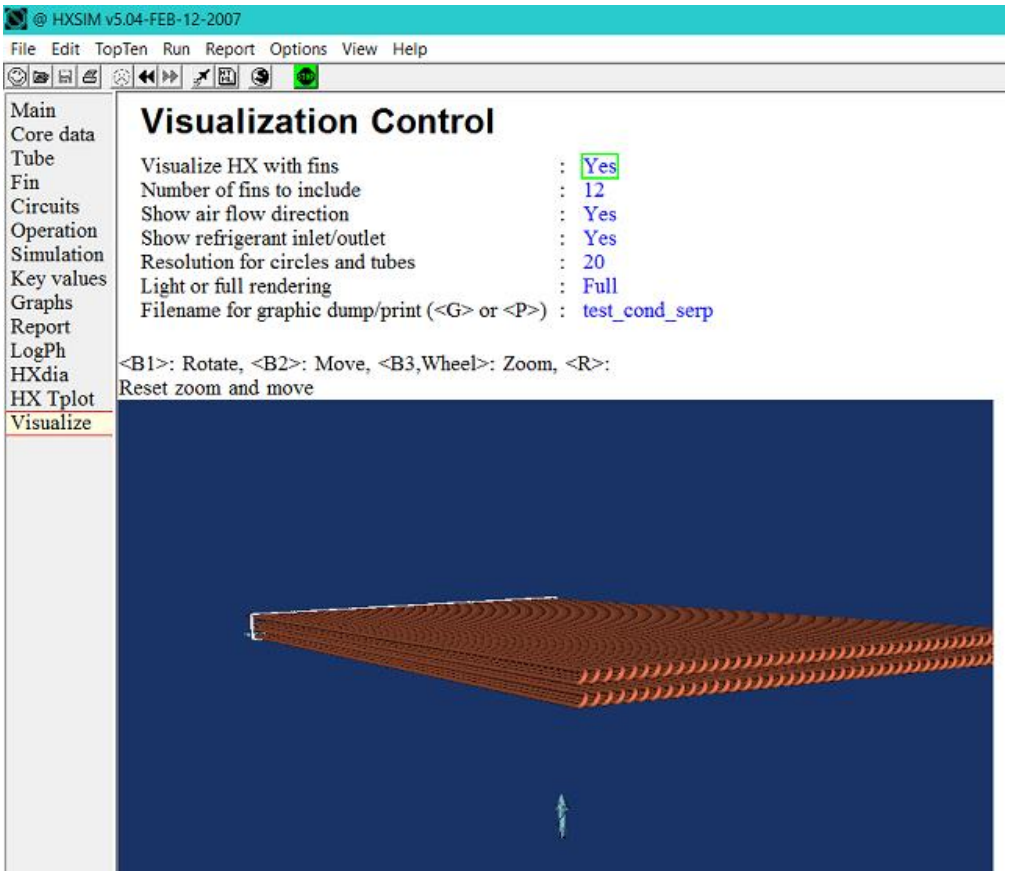

Figure 5.3 Visualisation of projected heat exchanger in hXSIM

5.2 Adopted assumptions to the simulations

Technical data of currently working Transcritical Gas Cooler – 50 Hz (unit type: Alfablue Double row) were simulated to determine appropriate fin enhancement factor and fin efficiency. This factors were later used throughout all simulations. The main results of this simulation are presented in Appendix A along with the values of fin enhancement factor and fin efficiency (marked in yellow).

Simulations of divided gas cooler were carried out with following assumptions:

- inlet air temperatures varies from -15 to 15°C with 5 K intervals
- in the first part of the gas cooler the maximum rpm of fans cannot be higher than the maximum volumetric flow rate of two fans (i.e. 5.66 m^3/s), whereas in the second part the fan should run with a considerably lower flow rate, that is also lower than the maximal flow rate of one fan (i.e. 2.83 m^3/s)
- refrigerant flow depends on the frequency of MT-compressors, which changes from minimum (30 Hz) to maximum (60 Hz); the compressors work in a scope of 8÷50% of total capacity

- inlet refrigerant temperature is set to 40°C or 60°C (in some cases even higher)
- inlet refrigerant pressure is generally set to 55 bar, but in order to meet demands of the gas cooler and compressors (pressure rises gradually along with the inlet air temperature) this figure fluctuates between 54 bar and 68 bar
- refrigerant after the first part of the gas cooler should be liquid and subcooled by at least 1 K
- liquid refrigerant after the first part should be subcooled further, but cannot obtain temperature lower than 5°C, so that suitable pressure range inside the liquid separator is ensured

5.3 Procedure of simulations

1) First of all, maximum and minimum refrigerant flow is to be determined. To achieve that following technical data regarding MT-compressors are used:

- Compressor 1: Displacement: 4.74 m^3/h at 50 Hz
- Compressor 2: Displacement: 11.62 m^3/h at 50 Hz
- Compressor 3: Displacement: 13.84 m^3/h at 50 Hz

As it was already mentioned each frequency controlled compressor (number one and number two) works between the range of 30÷60 Hz. The operating range for MT-compressors assumed in simulations is shown in Tab. 2.

Table 2 Range of work and adjustments of MT-compressors (Herdlitschka, 2016)

Range of work, %	Number of MT-compressor
8÷17	1
17÷22	gap
22÷42	2
28÷50	1+2

On the grounds of above mentioned data, mass flow rates for the whole range of work are to be determined. Exemplary calculation for the first range of work (8÷17%) are presented below, and the results for other scopes are presented in Appendix B.

Owing to the fact that minimal and maximal frequency are known, the whole range of frequency was calculated by the application of linear interpolation, e.g., for 9%:

$$f = 30 + \frac{60-30}{17-8} \cdot (9-8) \tag{5}$$

Considering that displacement for 50 Hz equals 4.74 m^3/h, other displacement fluxes were calculated using simple proportion, e.g., for 33.3 Hz:

$$\dot{V}_d = \frac{4.74 \cdot 33.3}{50} \tag{6}$$

Lastly, refrigerant mass flow rates were calculated using the volumetric efficiency of the compressor:

$$\eta_V = \frac{\dot{m} \cdot v}{\dot{V}_d} \rightarrow \dot{m} = \frac{\eta_v \cdot \dot{V}_d}{v} \tag{7}$$

where: ṁ - refrigerant mass flow rate [kg/s], v – specific volume of the refrigerant at compressor inlet (for set temperature -5°C it is equal to 0.01201 m^3/kg), η_v - volumetric efficiency (assumed to be equal to 0.75)

Final results are presented in Tab. 3.

Table 3 Refrigerant flow rates for the MT-compressors, range of work 8÷17%

Scope of work, %	Frequency, Hz	Displacement, m^3/h	Mass flow, kg/s
8	30	2.84	0.049
9	33.3	3.16	0.055
10	36.7	3.48	0.060
11	40	3.79	0.066
12	43.3	4.11	0.071
13	46.7	4.42	0.077
14	50	4.74	0.082
15	53.3	5.06	0.088
16	56.7	5.37	0.093
17	60	5.69	0.099

To conclude, the maximal refrigerant flow is equal to 0.341 kg/s, whereas the minimal refrigerant flow is tantamount to 0.049 kg/s. This values are used throughout all simulations as boundary conditions.

2) Secondly, compressors power demand and theoretical fan power demand is to determined.

Theoretical fan power demand is computed by hXSIM in every simulation. Nevertheless, this estimation is not accurate since the total nominal power for 6 fans has to be (according to the manufacturer) 1260 W, which gives 210 W for each blower. Thus, each value computed by hXSIM has to be multiplied by 2.78 in order to get more accurate result.

To justify application of higher (than standard 55 bar) refrigerant pressure an estimation of compressors power demand is to be determined. Assuming that isentropic efficiency equals 0.65, compressors power [kW] equals:

$$P_{COMP} = \frac{\dot{m} \cdot (h_{2s} - h_1)}{\eta_{is}} \tag{8}$$

where: ṁ - refrigerant mass flow [kg/s], h_{2s} - isentropic specific enthalpy at the compressors outlet [kJ/kg] , h_1 - specific enthalpy at the compressors inlet [kJ/kg], η_{is} - isentropic efficiency

Calculations were carried for boundary conditions, i.e., maximal and minimal outlet pressure, along with maximal and minimal refrigerant flow that is projected for the compressors. To calculate values for pressures between maximum and minimum linear interpolation was applied. The results are presented in Tab. 4 and Fig. 5.4. Exemplary calculations for maximum flow and typical conditions (i.e. inlet: p = 30.5 bar; t = -5°C and outlet: 55 bar):

- $h_1 = f(p_1 = 30.5; t_1 = -5) = 433.46$ kJ/kg
- $h_{2s} = f(p_2 = 55; s_{2is} = s_1 = 1.87) = 455.66$ kJ/kg
- $P_{COMP} = \frac{0.3405 \cdot (455.66 - 433.46)}{0.65} = 11.63$ kW

Table 4 MT-compressors power demand for different pressures

Outlet pressure, bar	Power demand for maximal flow, kW	Power demand for minimal flow, kW
55	11.63	1.68
56	11.99	1.73
57	12.36	1.79
58	12.72	1.84
59	13.08	1.89
60	13.45	1.95
61	13.81	2.00
62	14.17	2.05

63	14.53	2.10
64	14.90	2.16
65	15.26	2.21
66	15.62	2.26
67	15.99	2.32
68	16.35	2.37

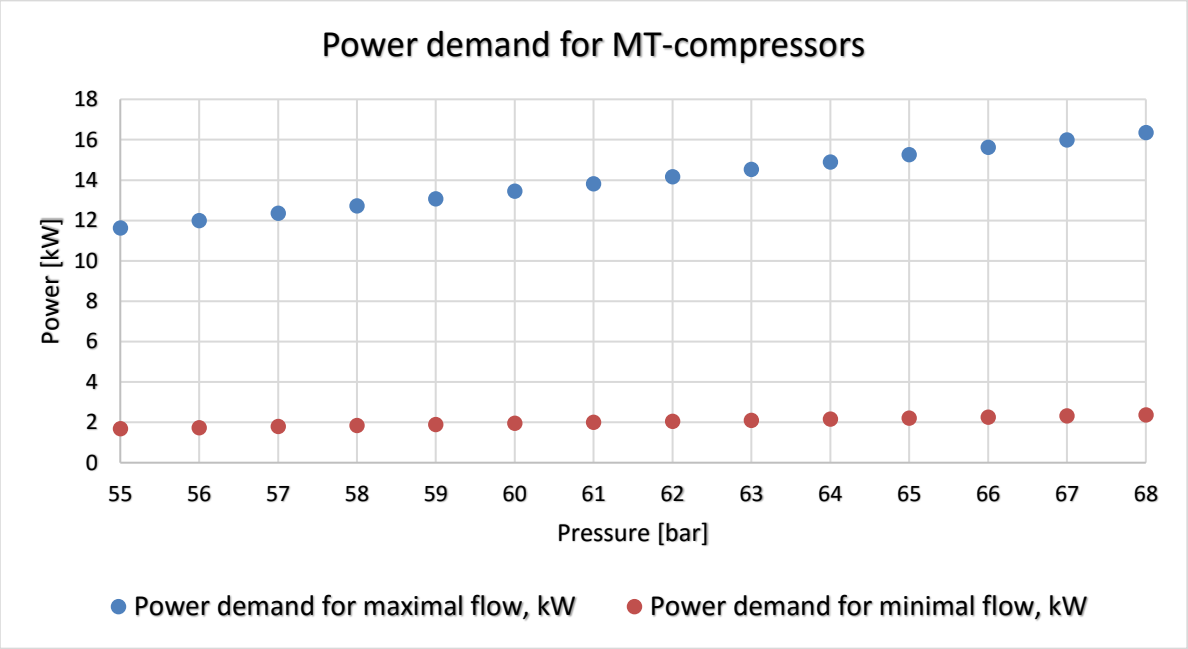

Figure 5.4 Power demand for MT-compressors for different pressures

To sum up, increasing the GC outlet pressure by 1 bar requires on average:

- for maximal flow 0.36 kW ,
- for minimal flow 0.05 kW.

Thereby, increasing the GC outlet pressure is more advantageous for low refrigerant flows.

3) Simulations in hXSIM of the first part of the gas cooler

The aim of this simulations is to achieve a slightly subcooled (by 1 K) liquid CO_2 at the GC outlet, which is projected to be used later in the second part of the GC. The simulations intent to use the lowest possible air flow rate, which means also the lowest power demand for the fans. As it was already mentioned, the first part encompasses one third of the total length (i.e. finned tube length 2100 mm) and two blowers, which are able to work with maximal flow rate equal to 5.66 m^3/s. In two cases refrigerant inlet temperature (and pressure) is increased owing to the fact that projected temperature (20°C) is too low to achieve 1 K of subcooling at

those pressures levels within fans working range. Simulations provided outlet parameters for different boundary conditions, thus it is possible to depict overall working range for the fans (shown in Fig. 5.5). All input and output data are presented in Tab. 5.

Table 5 Results from simulations of the first part of the gas cooler

Inlet refr. temp., °C	60								20			25	20			25
Inlet refr. press., bar	55	55	60	68	55	55	55	60	55	55	56	64	54	55	57	60
Refr. flow, kg/s	0.3405				0.0493				0.3405				0.0493			
Inlet air temp., °C	-15	-5	5	15	-15	-5	5	15	-15	-5	5	15	-15	-5	5	15
Air flow rate, m^3/s	1.63	2.967	4.4	5.2	0.1573	0.2427	0.5068	1.16	1.2205	2.058	4.56	5.4	0.156	0.225	0.352	0.93
Performance, kW	82.7	82.7	76.7	68	11.98	11.98	11.98	11	58.5	58.5	56.3	43.9	8.79	8.47	7.8	7.8
Outlet refr. temp., °C	17.23	17.22	21.03	26.5	17.23	17.22	17.22	21.07	17.22	17.22	18.06	23.75	16.3	17.21	18.8	21.02
Refrigerant content (liquid), kg	13.65	13.66	13.02	11.87	13.66	13.66	13.66	13.01	13.66	13.66	13.52	12.51	13.80	13.66	13.40	13.03
Fan power demand, W	51.07	251.8	716.2	1105.6	0.08	0.3	2.1	19.5	23.5	94.05	788.7	1223.9	0.08	0.25	0.8	10.8

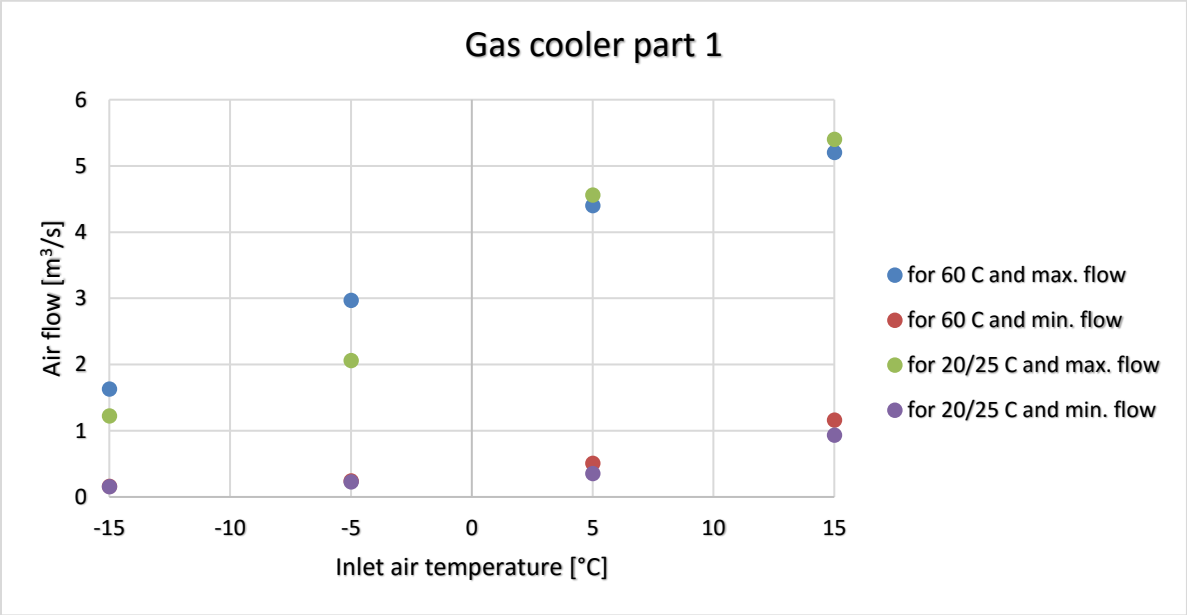

Figure 5.5 Fans air flow rate vs. inlet air temperature for different inlet parameters, GC part 1

An estimation of fans power demand in relation to air flow rates is depicted in Fig. 5.6.

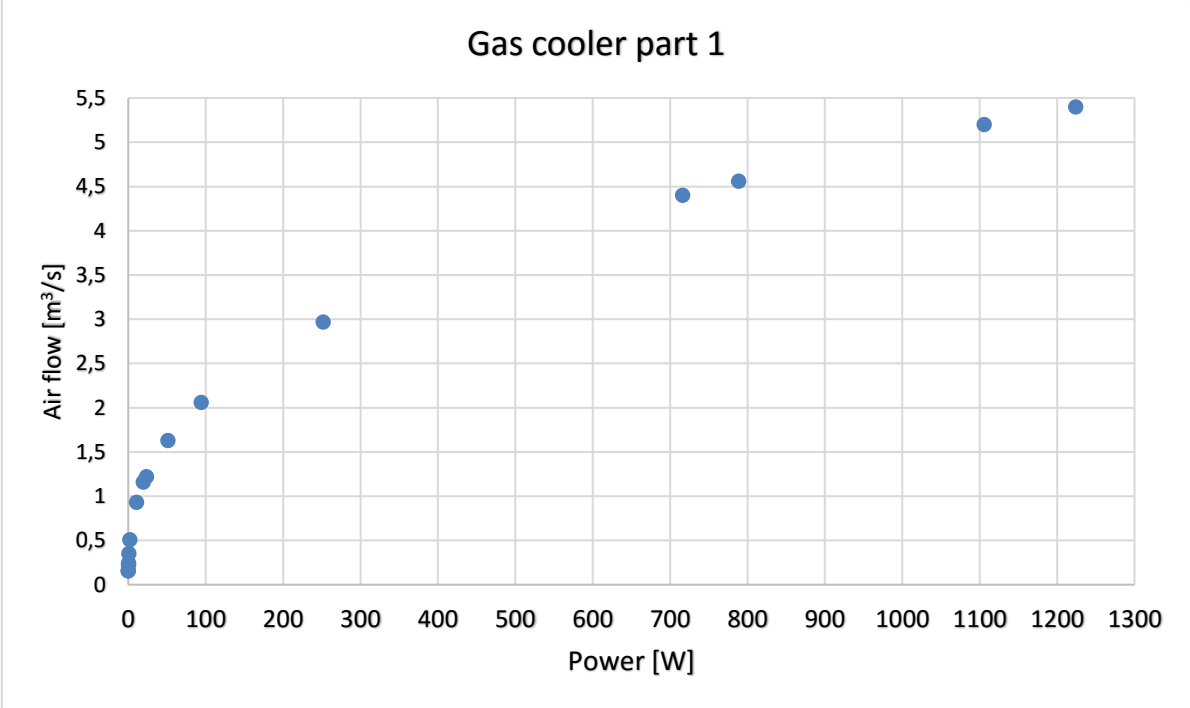

Figure 5.6 Fans air flow rate vs. Fans power demand, GC part 1

To summarize, on the basis of calculations and graphs it can be noticed that:

- air flow rate increases nearly linearly with the increase in ambient air temperature

- refrigerant's outlet temperature amounts to, averagely, around 19°C
- fans power demand increases with the increase in air flow rate; an average power demand equals 268 W
- refrigerant content (liquid) amounts to, averagely, around 13.3 kg
- an average air flow rate is much lower than maximal flow rate for two fans and is equal to 1.95 m^3/s

4) Simulations in the hXSIM of the second part of the gas cooler

The purpose of this simulations is to obtain refrigerant outlet temperature within acceptable range that is appropriate for liquid separator's pressure level (i.e. not lower than 5°C). To achieve this temperature, very low air flow rates are utilised, thus creating approximately natural convection. The second part of the gas cooler consists of two thirds of the total length (i.e. finned tube length 4200 mm), and one fan that is able to work with maximum volumetric flow rate equal to 2.83 m^3/s. The whole working range for the fan is shown in Fig. 5.7. Simplified p-h diagram, shown in Fig. 5.9, portrays the GC outlet parameters within acceptable range, which are the results of simulations. All input and output data are shown in Tab. 6.

Table 6 Results from simulations of the second part of the gas cooler

Inlet refr. temp., °C	17.23	17.22	21.03	26.5	17.23	17.22	17.22	21.07	17.22	17.22	18.06	23.75	16.3	17.21	18.8	21.02
Inlet refr. press., bar	55	55	60	68	55	55	55	60	55	55	56	64	54	55	57	60
Refr. flow, kg/s	0.3405				0.0493				0.3405				0.0493			
Inlet air temp., °C	-15	-5	5	15	-15	-5	5	15	-15	-5	5	15	-15	-5	5	15
Air flow rate, m^3/s	0.16	0.29	0.6	0.65	0.019	0.031	0.22	0.27	0.16	0.29	0.6	0.65	0.018	0.031	0.24	0.28
Performance, kW	11.8	12.2	13.3	10.6	1.7	1.7	1.7	1.06	11.8	12.2	10.6	7.9	1.6	1.7	2	1
Outlet refr. temp., °C	5.47	5	8.73	19.12	5.14	5.12	5.12	15.03	5.46	5	7.86	17.84	5	5.1	5.1	15.03
Refrigerant content (liquid), kg	29.48	29.59	28.9	26.4	29.56	29.56	29.56	27.21	29.49	29.59	28.97	26.56	29.56	29.57	29.63	27.22
Fan power demand, W	0.028	0.17	1.06	1.28	0.0001	0.0004	0.083	0.1	0.03	0.17	1.06	1.28	0.00009	0.0004	0.08	0.14
Temperature approach, K	20.47	10	3.73	4.12	20.14	10.12	0.12	0.03	20.46	10	2.86	2.84	20	10.1	0.1	0.03
Q-difference, kW	8.49	10.27	-	-	1.36	1.54	-	-	8.48	10.26	-	-	1.25	1.54	-	-
Deviation, %	29.3	20	-	-	43.5	40.6	-	-	29.3	20	-	-	43.8	40.6	-	-

Q-difference denotes the difference in final overall heat balance between refrigerant side and air side. Performance indicates actual heat transfer rate in the GC, i.e., heat transfer on the refrigerant side. Deviation, on the other hand, designates the percentage difference in enthalpy between circuits. Empty spaces in the section (in Tab. 6) Q-difference and deviation imply negligible (typical) difference in heat balance, i.e., less than 2% of deviation between circuits.

Temperature approach points out the difference between the GC outlet refrigerant temperature and inlet air temperature. Low temperature approach implies higher dimensions, i.e. more heat transfer area is required, and thus higher costs. If the temperature approach dropped to a value lower than zero, the heat transfer would cease.

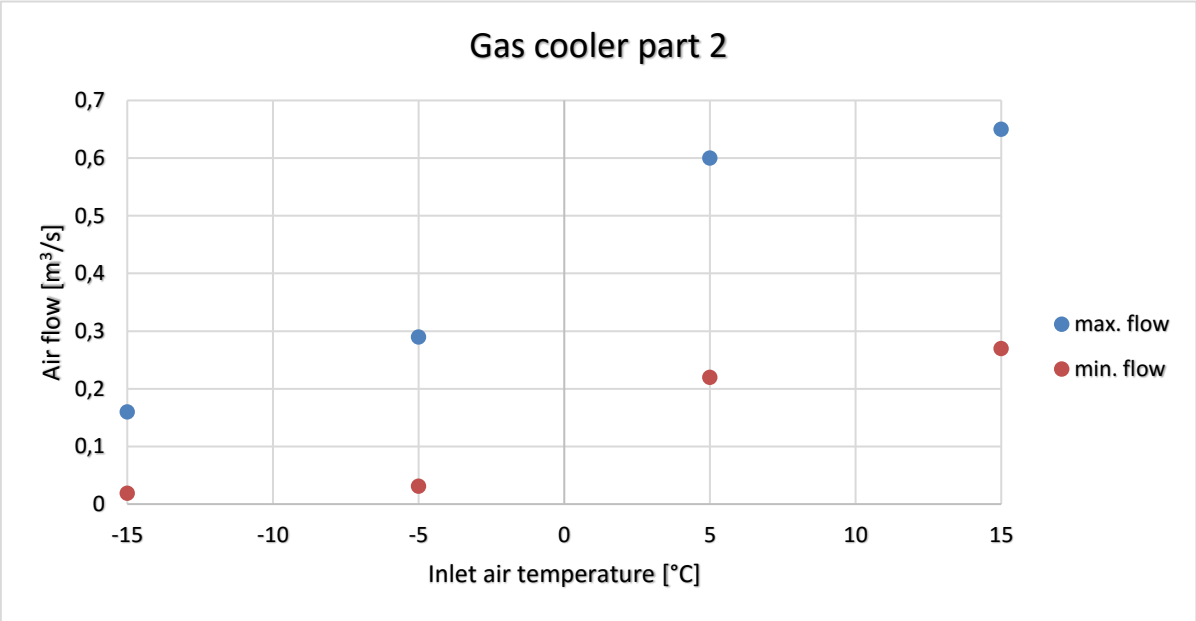

Figure 5.7 Fan air flow rate vs. inlet air temperature for different inlet parameters, GC part 2

An estimation of fan power demand is depicted in Fig. 5.8.

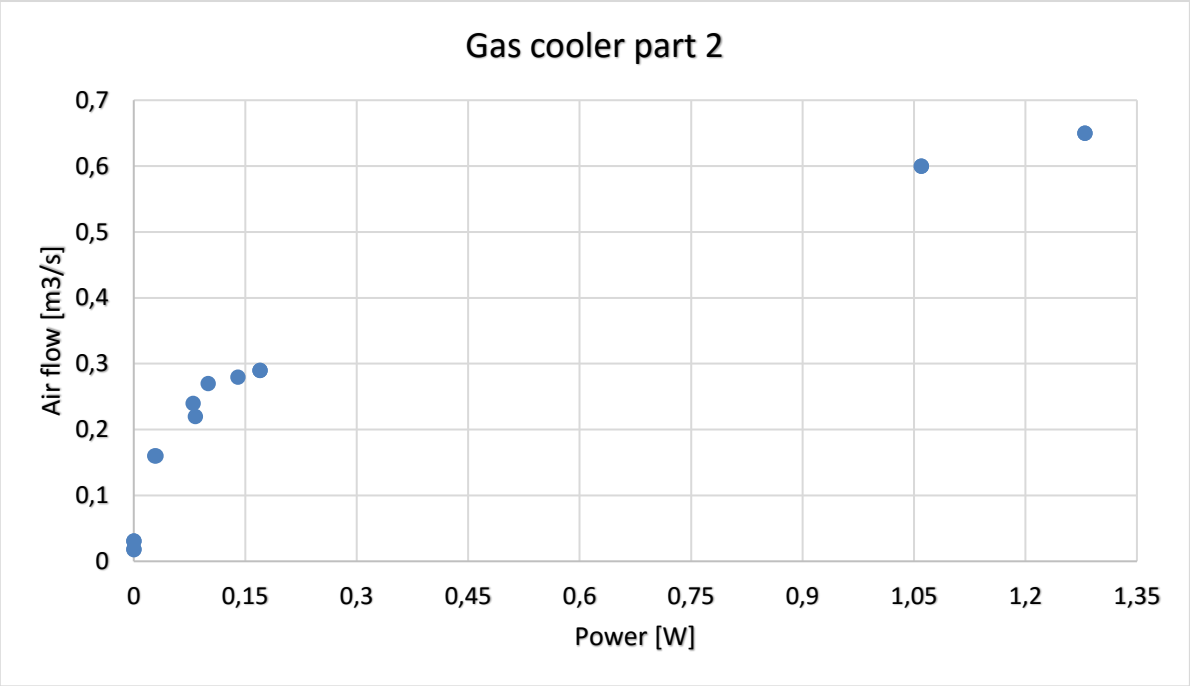

Figure 5.8 Fan air flow rate vs. Fan power demand, GC part 2

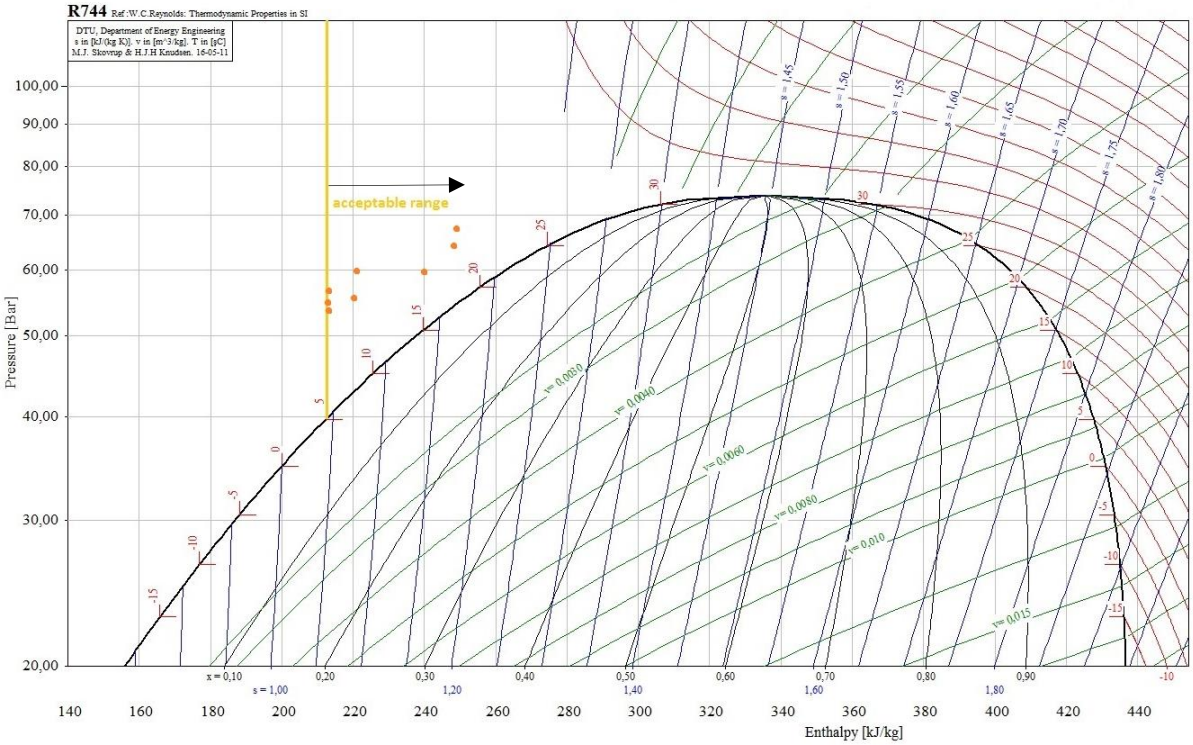

Figure 5.9 Simplified p-h diagram with acceptable gas cooler outlet parameters (yellow line) with calculated output values (orange dots)

To sum up, on the basis of calculations and graphs it can be noticed that:

- in few cases heat balance is disregarded in order to reach aimed refrigerant outlet temperature, thus occurs considerable heat loss to the surroundings

- air flow rate increases with the increase in ambient air temperature
- refrigerant outlet temperature amounts to, averagely, around 8.5°C
- fan power demand increases with the increase in air flow rate; an average power demand is equal to 0.34 W
- refrigerant content (liquid) amounts to, averagely, around 29 kg
- an average air flow rate is much lower than maximal flow rate for one fan and equals 0.28 m^3/s

6. IMPROVEMENTS IN THE ONGOING SYSTEM IN REMA 1000 PRINSENSGATA

The system working in Rema 1000 Prinsensgata was amended in order to keep the system in more stable conditions. Following changes were implemented by Danfoss, Enex and Trondheim Kulde:

1) Installation of a shut-off valve for the gas cooler

A shut-off valve for the GC reduces the capacity by 50% when the ambient temperature is lower than 7°C. Due to this enhancement controlling of the high-side parameters should be easier, thus system should work more stable. A picture of the gas cooler with a shut-off valve is shown in Fig. 6.1.

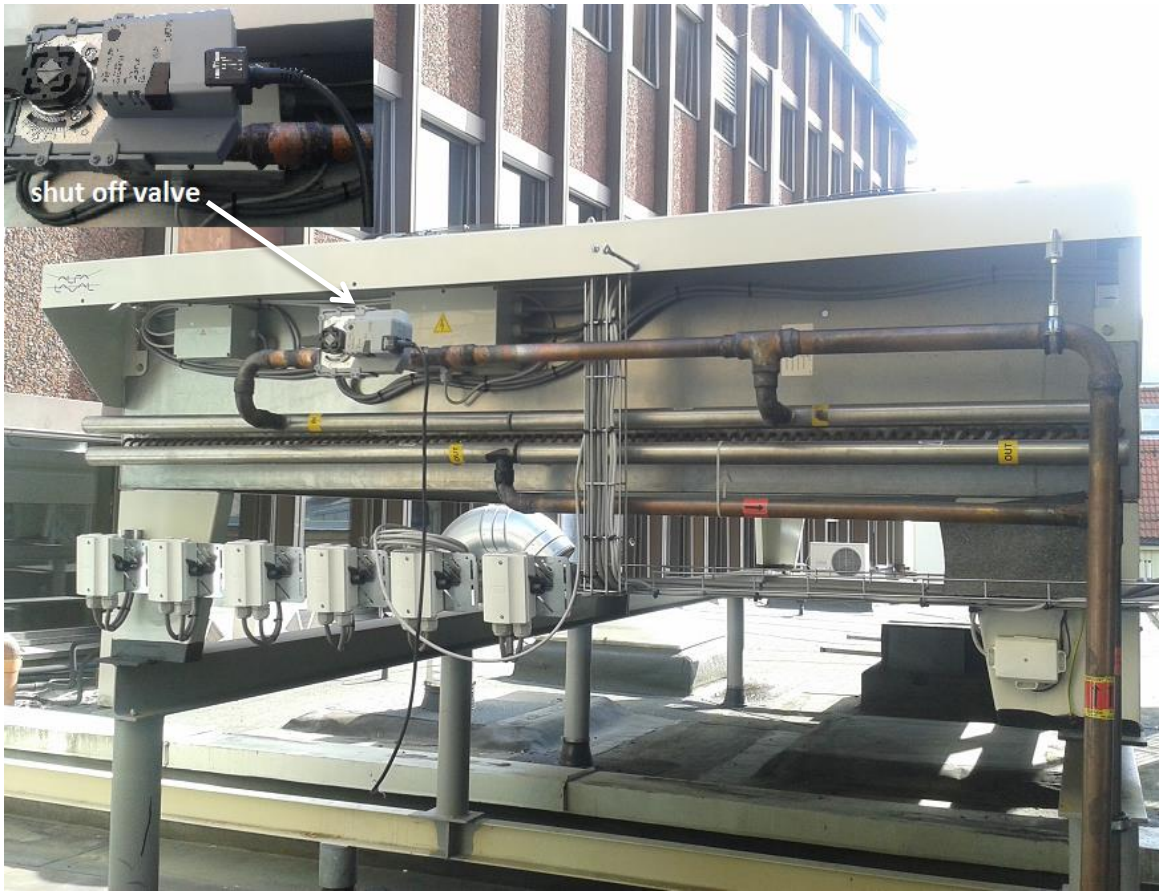

Figure 6.1 Gas cooler with a shut-off valve

2) Reprogramming gas cooler's fans

Gas cooler's fans are programmed to work in certain ranges (shown in Fig. 6.2) which depends on the refrigerant outlet temperature and the ambient temperature. Additionally, the gas cooler,

equipped with a shut-off valve, closes 50 percent of the GC if the ambient temperature is lower than 7°C. In case of that situation only fans 1÷3 are in operation (depicted in Fig. 6.2) since fans requested capacity is expected to be lower than 60%, hence signal generated by external device for the fans amounts to maximum 6 V. Above 7°C all fans may be in operation, especially during periods of high load of system, i.e., during summertime.

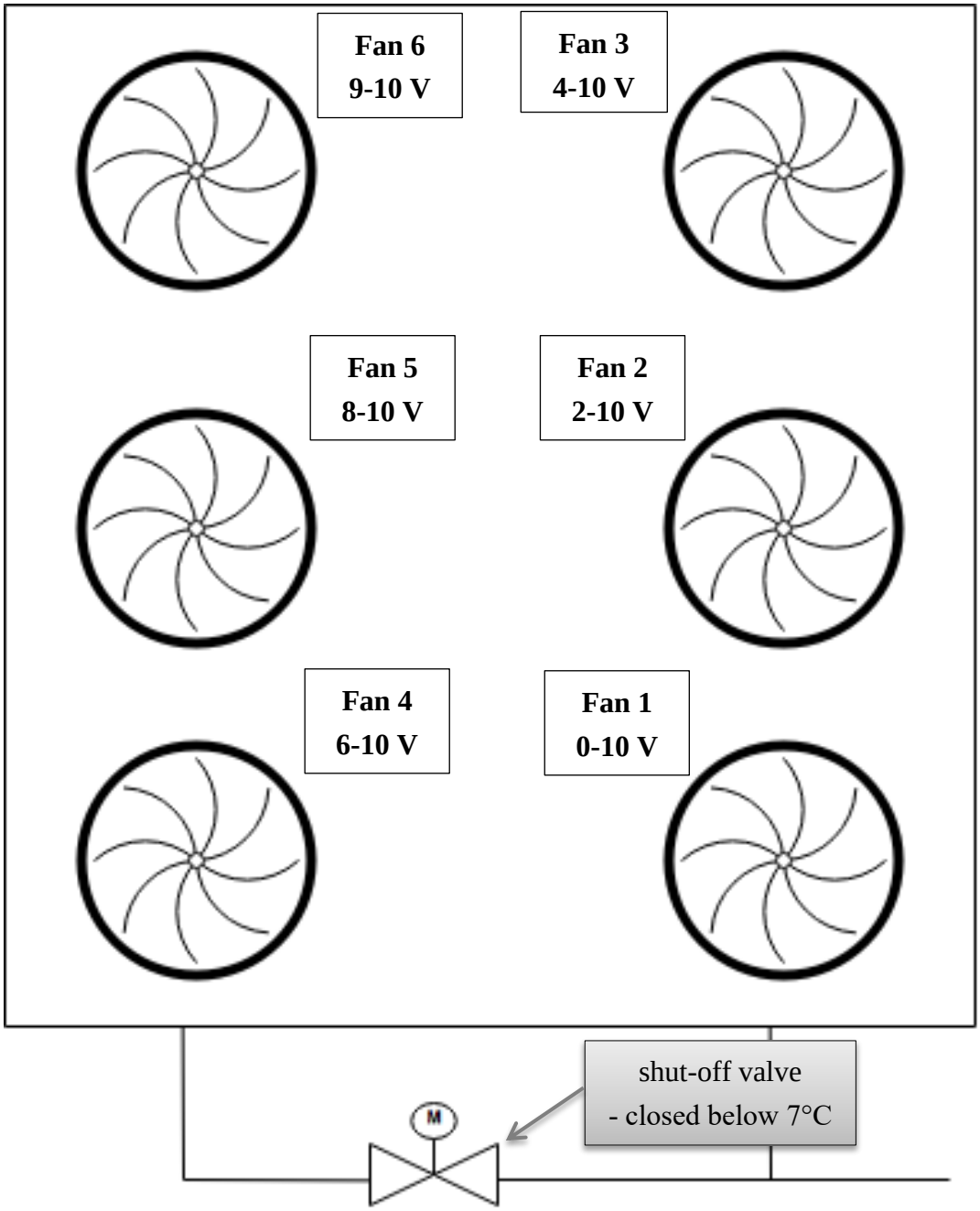

Figure 6.2 Gas cooler's fans after reprogramming

3) Signals from all energy meters were reconfigured and connected to the system's acquisition program

After this amendment energy consumption is visible (available) online in StoreView, which is a data acquisition program provided by Danfoss, designed to collect all measured parameters in the system. To check if the total energy consumption presented in StoreView is in line with actual values which appear on energy meters mounted in Rema 1000, a comparison was made between data from energy meters located at Prinsensgata (presented in Tab. 7) and data collected by StoreView (shown in Tab. 8). Tables depict data collected from seven different energy meters during three randomly selected days. Energy meter denoted snow-melting-unit means heat rejected towards street heat exchangers, thus streets dry up (after rainfalls and snowfalls) much quicker compared to other areas.

Table 7 Data from energy meters collected in Rema 1000

	Total energy consumption, kWh		
Energy meter	July 5, 15:16	July 6, 11:49	July 8, 10:52
Heat recovery	27263	27489	27991
AC-evaporator	1801	1801	1803
AHU-heater	11885	11885	11885
Snow-melting-unit	12328	12555	13038
MT-Compressors	30300.6	30462.9	30806.1
LT-Compressors	2633	2645.6	2672.3
AUX-Compressors	2261.1	2263.2	2264.4

Table 8 Data from energy meters collected by StoreView

	Total energy consumption, kWh		
Energy meter	July 5, 15:16	July 6, 11:49	July 8, 10:52
Heat recovery	5451.9	5681.6	6183.6
AC-evaporator	942.7	942.7	942.7
AHU-heater	372.3	372.3	372.3
Snow-melting-unit	4329.6	4559.9	5042.9
MT-Compressors	30300.2	30462.9	30805.9
LT-Compressors	2632.6	2645.6	2672.1
AUX-Compressors	2260.8	2262.8	2264.3

The mean values of energy consumption measured in Rema 1000 (shown in Tab. 7) and collected by StoreView (shown in Tab. 8) are presented in following graphs:

1) Fig. 6.3 depicts a comparison of heat recovery's energy consumption

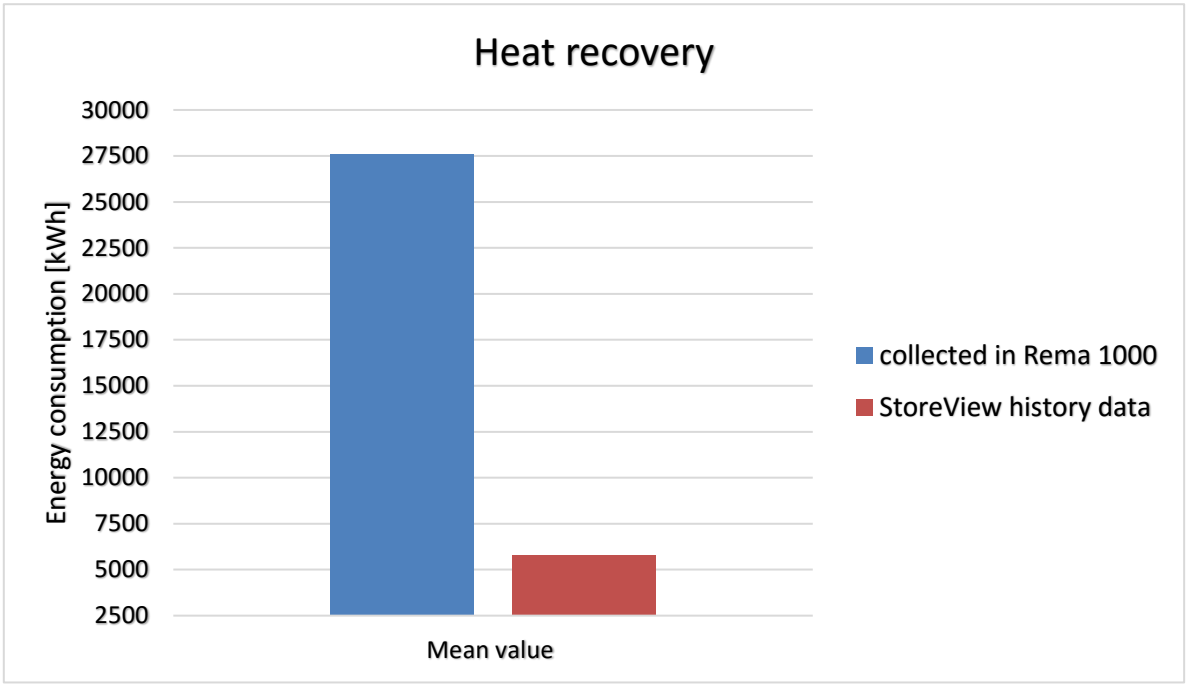

Figure 6.3 Comparison of heat recovery's energy consumption

2) Fig. 6.4 shows a comparison of AC–evaporator's energy consumption

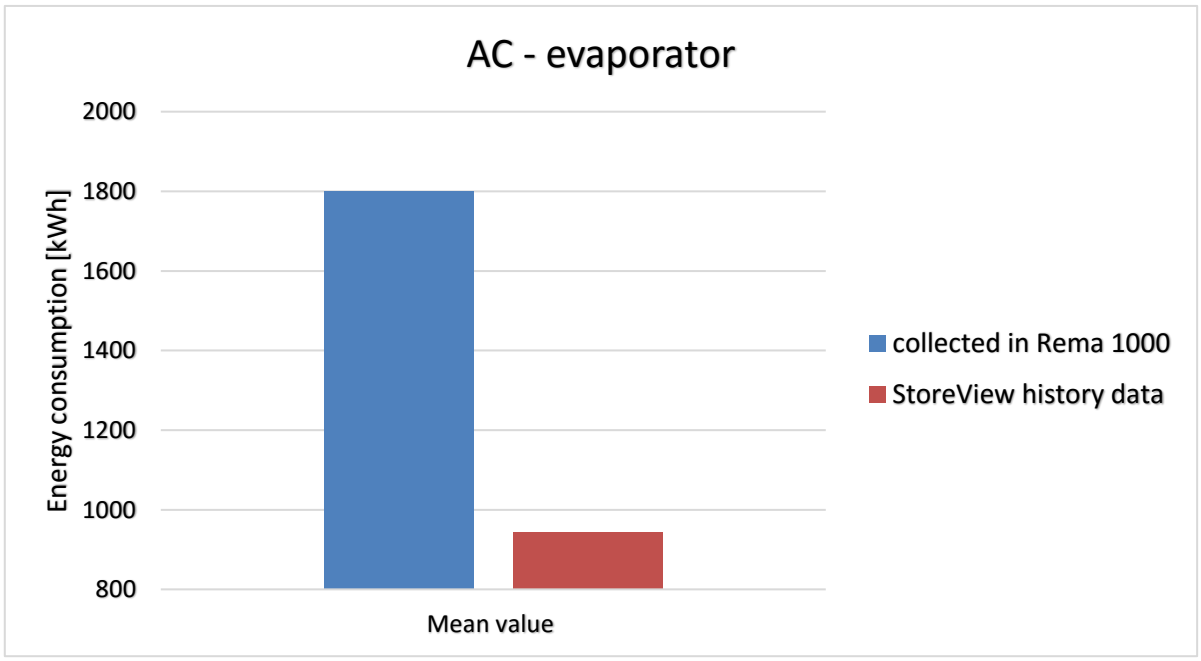

Figure 6.4 Comparison of AC–evaporator's energy consumption

3) Fig. 6.5 presents a comparison of AHU–heater's energy consumption

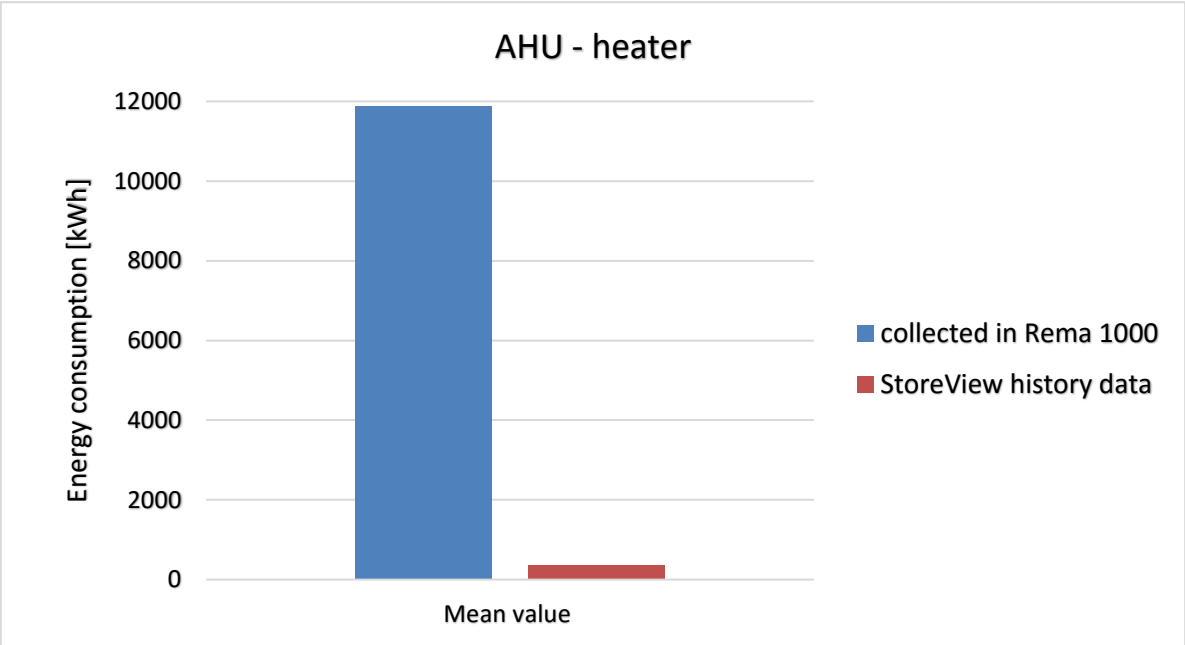

Figure 6.5 Comparison of AHU-heater's energy consumption

4) Fig. 6.6 presents a comparison of snow-melting-unit's energy consumption

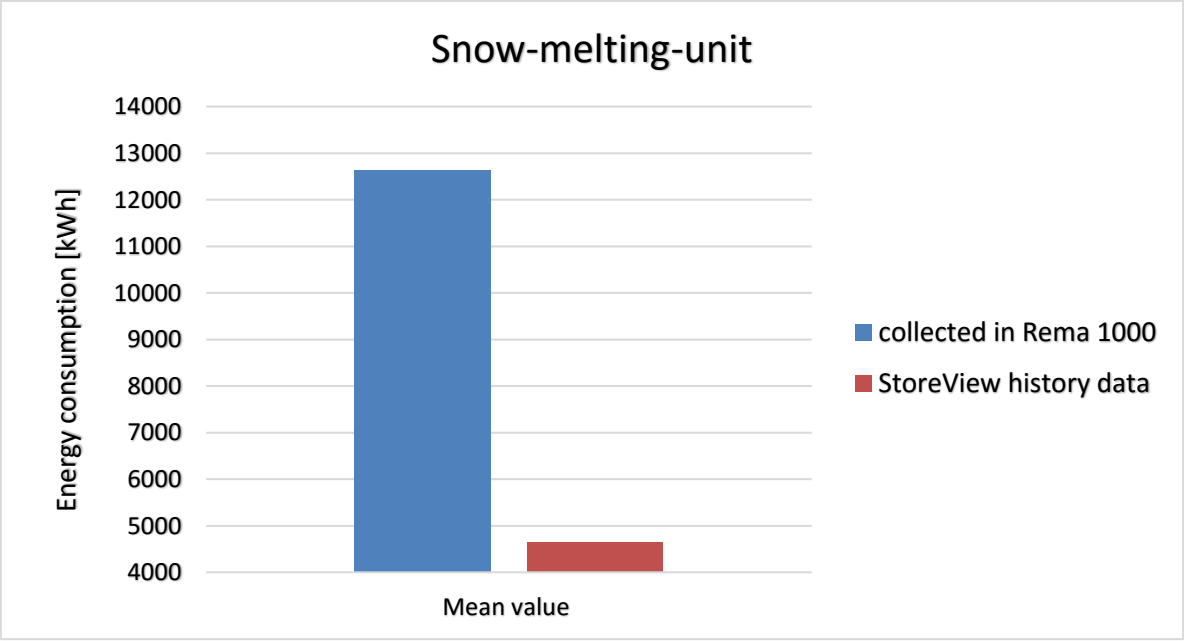

Figure 6.6 Comparison of snow-melting-unit's energy consumption

5) Fig. 6.7 presents a comparison of AUX-compressors' energy consumption

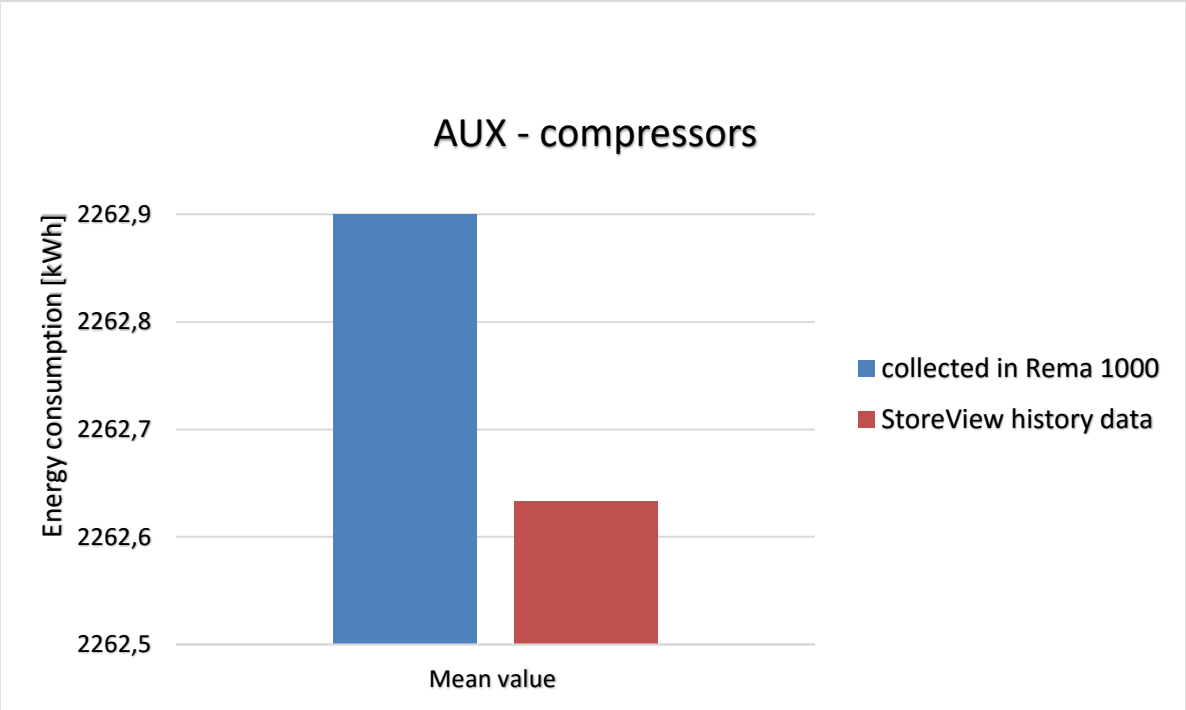

Figure 6.7 Comparison of AUX-compressors' energy consumption

6) Fig. 6.8 presents a comparison of LT-compressors' energy consumption

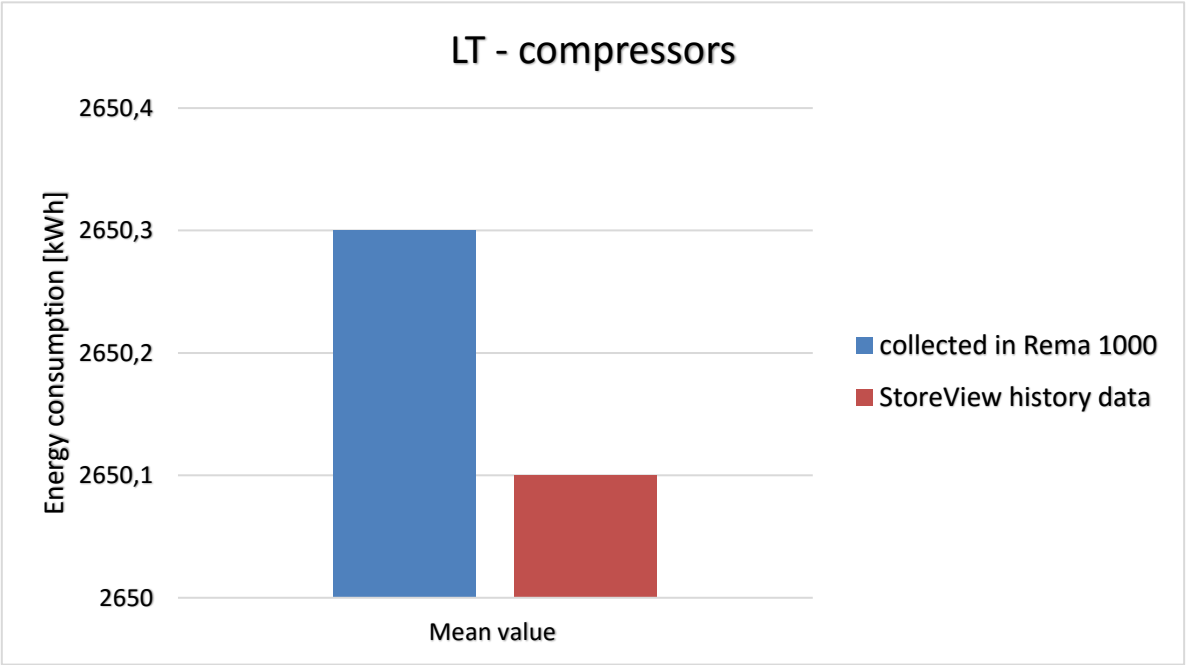

Figure 6.8 Comparison of LT-compressors' energy consumption

7) Fig. 6.9 presents a comparison of MT-compressors' energy consumption

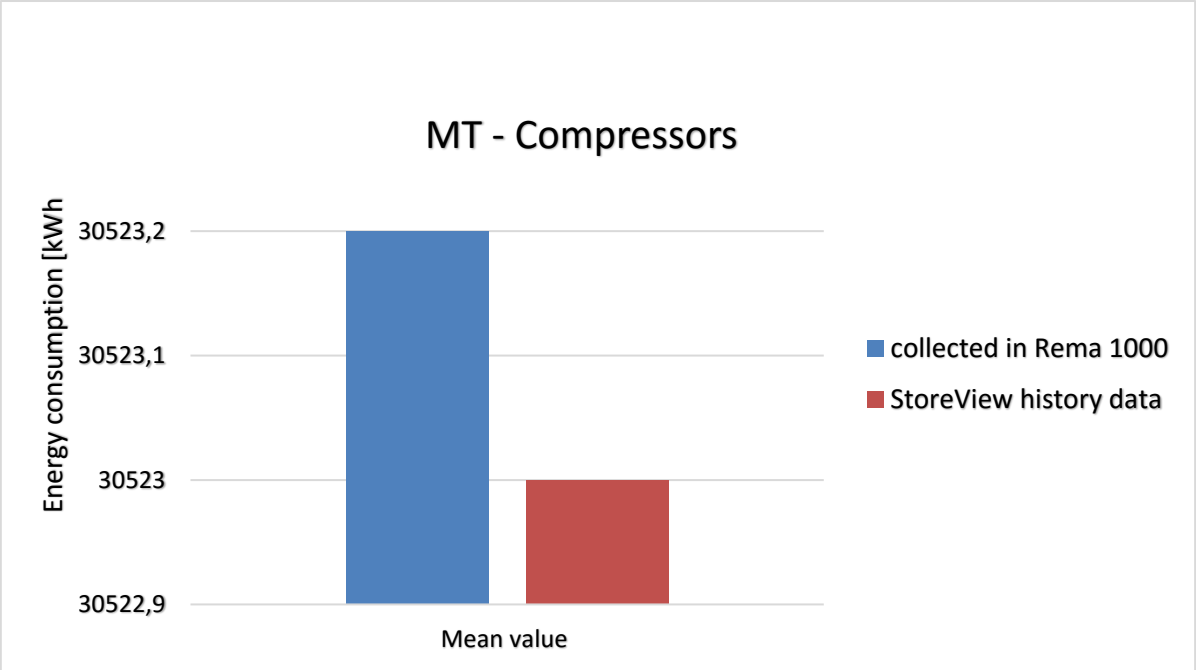

Figure 6.9 Comparison of MT-compressors' energy consumption

On the grounds of Fig. 6.3÷6.6, it can be noticed that there are significant discrepancies between values measured in Rema and data collected by StoreView. Nevertheless, energy consumption shown in Fig. 6.7÷6.9 proves that data presented in StoreView is correct since energy consumption is in this graphs practically the same (with negligible deviation).

In addition, a comparison of energy consumption between days was made to confirm that data recorded by StoreView are accurate (shown in Tab. 9).

Table 9 Differences between days in energy consumption

	Differences between days in energy consumption, kWh	
Energy meter	collected in Rema 1000	collected by StoreView
Heat recovery	226	229.7
	502	502
AC-evaporator	0	0
	2	0
AHU-heater	0	0
	0	0
Snow-melting-unit	227	230.3
	483	483
MT-Compressors	162.3	162.7
	343.2	343

LT-Compressors	12.6	13
	26.7	26.5
AUX-Compressors	2.1	2
	1.2	1.5

Finally, comparison of energy consumption between days for selected energy meters are presented in Fig. 6.10÷6.13 to demonstrate that StoreView data are accurate. Not all meters are depicted since the AC and AHU-heater practically did not work, or worked just a bit, during chosen days.

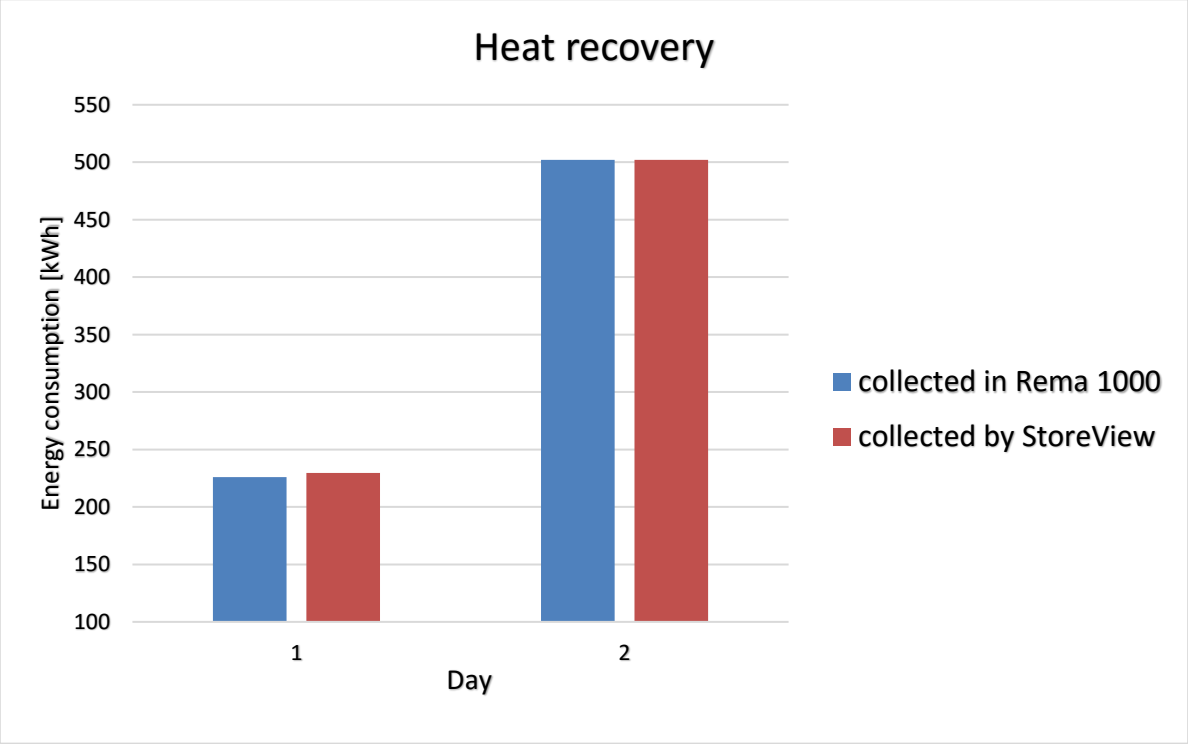

Figure 6.10 Differences between days of heat recovery's energy consumption

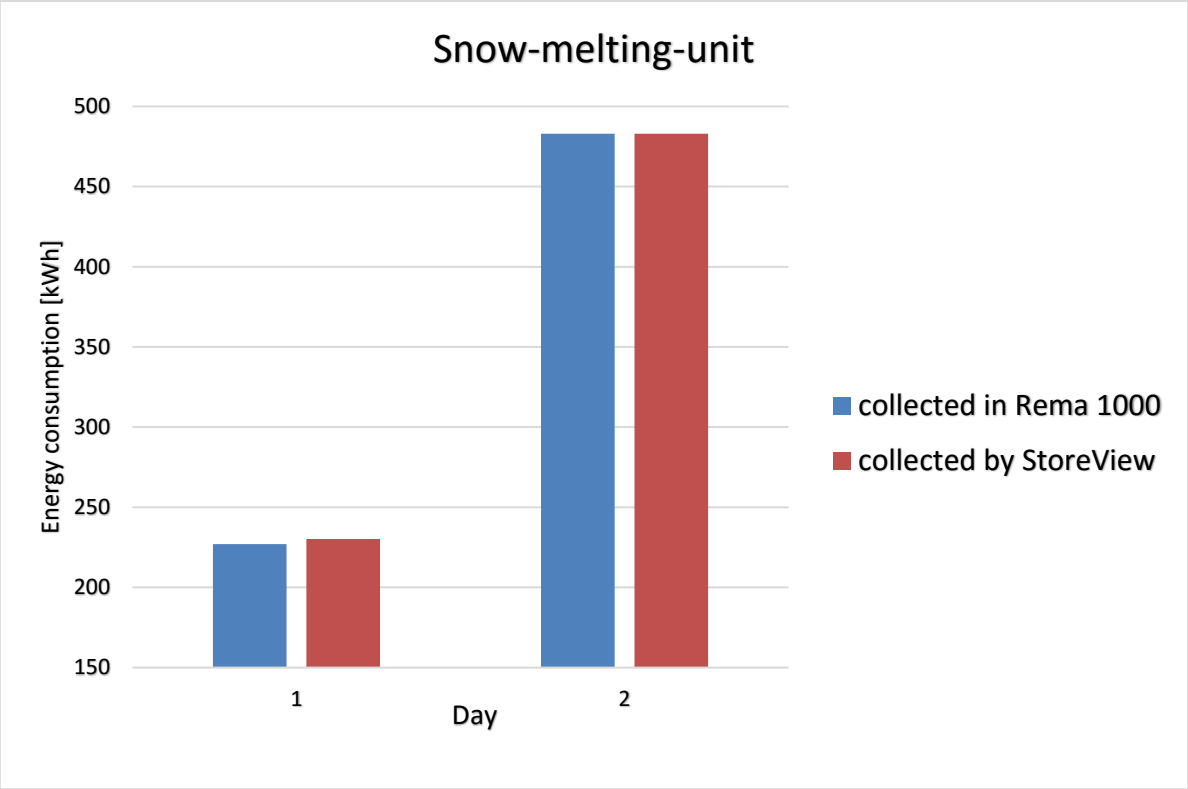

Figure 6.11 Differences between days of snow-melting-unit's energy consumption

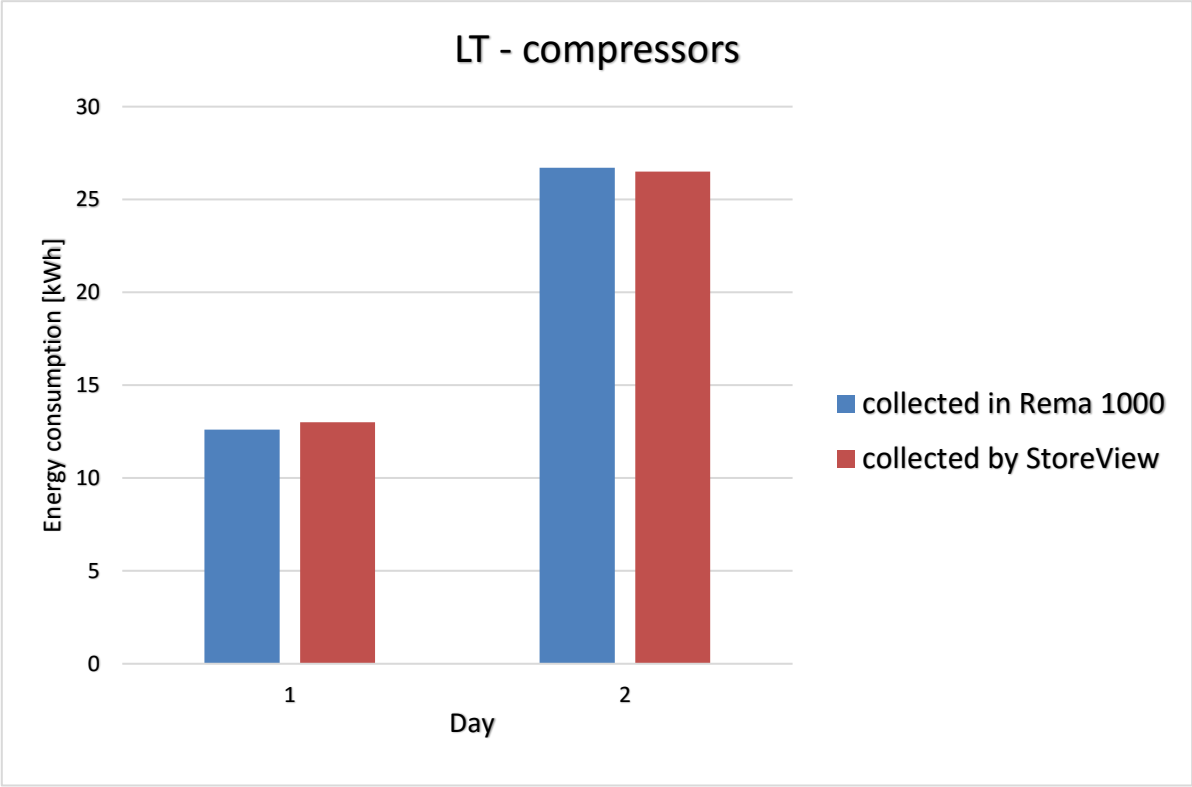

Figure 6.12 Differences between days of LT-compressors' energy consumption

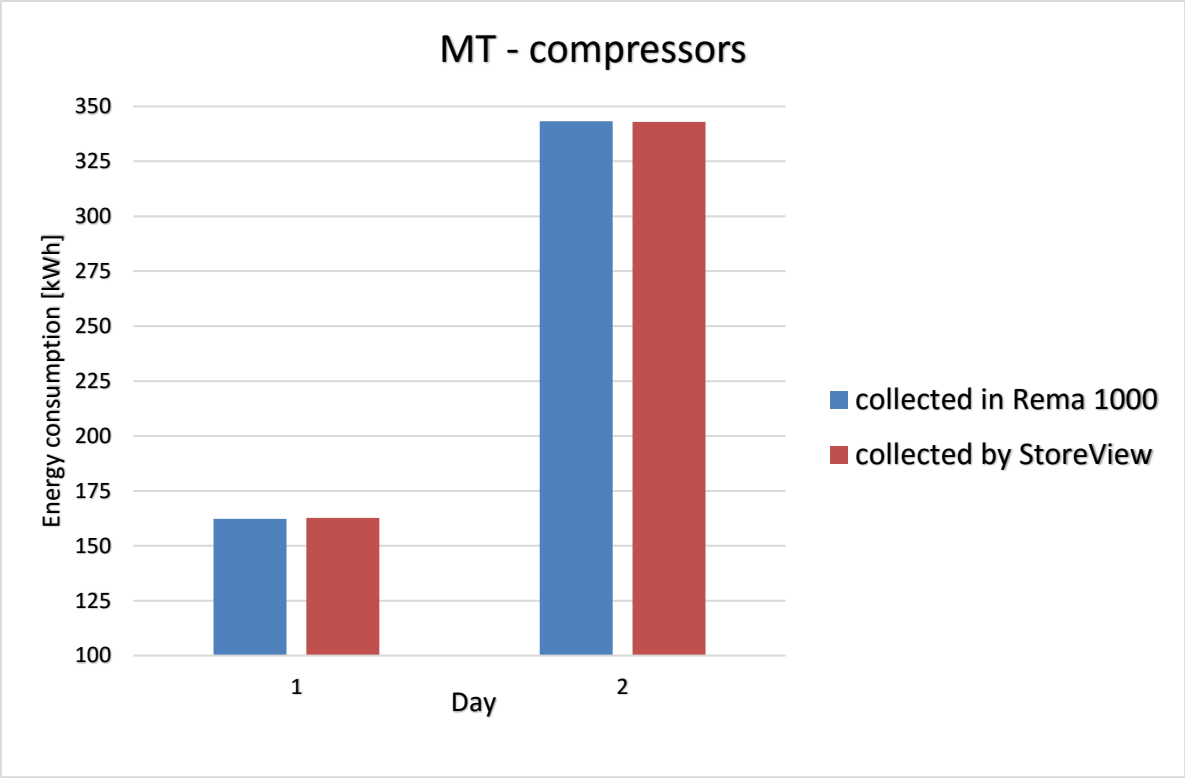

Figure 6.13 Differences between days of LT-compressors' energy consumption

4) Installation of a new pack controller for the ejectors

To evaluate the improvement of the system with the new pack controller, data (collected by StoreView) of few parameters depicting system's operation before and after the amendment is presented. Figures are portrayed in two variants with the air conditioning (AC) turned on or off. Fig. 6.14 and Fig. 6.15 present system in action before the installation of the new pack controller, whereas Fig. 6.16 and Fig. 6.17 show system's operation with the new pack controller.

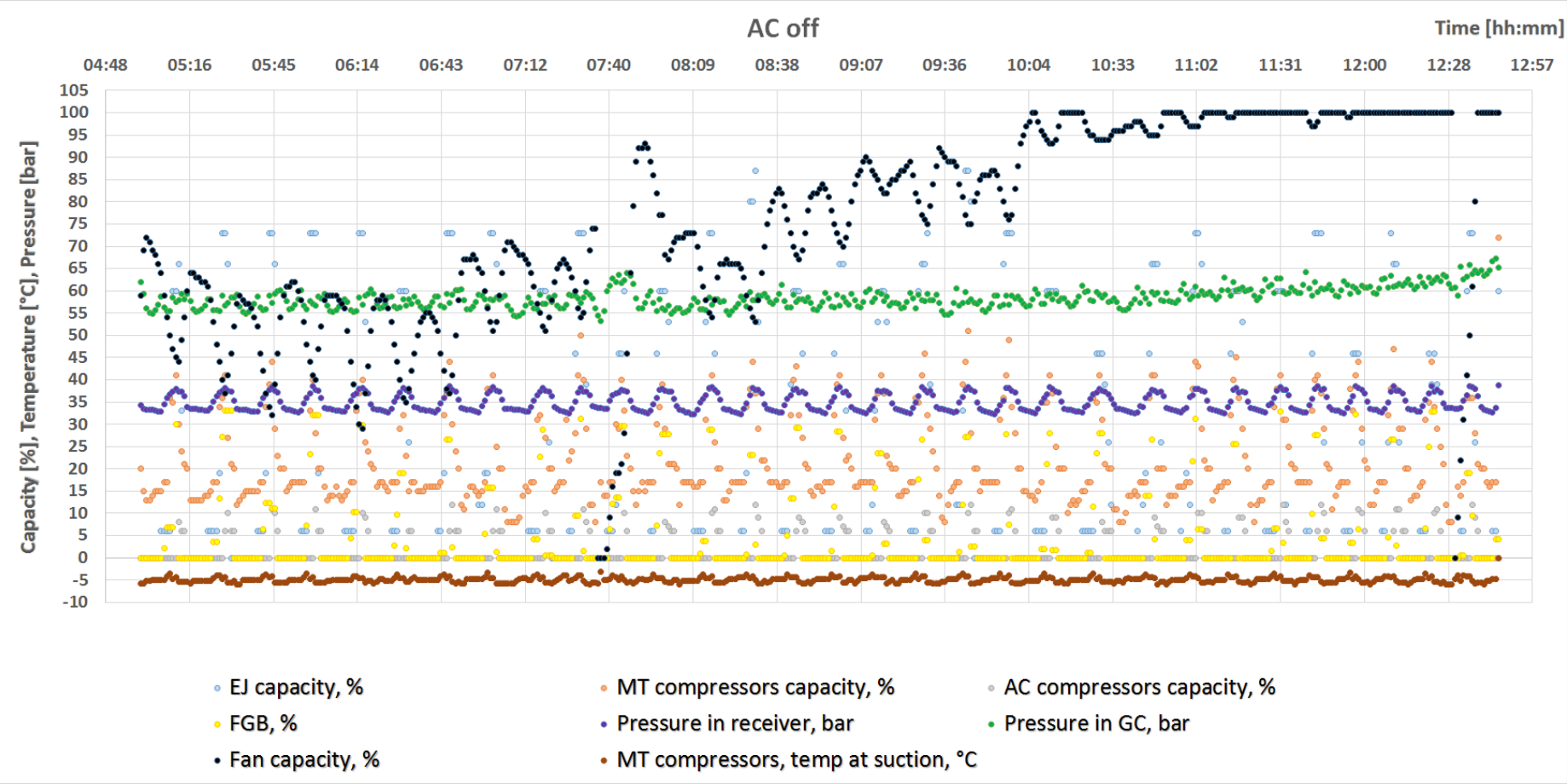

Figure 6.14 Refrigeration system in operation before the new ejector pack controller, AC off

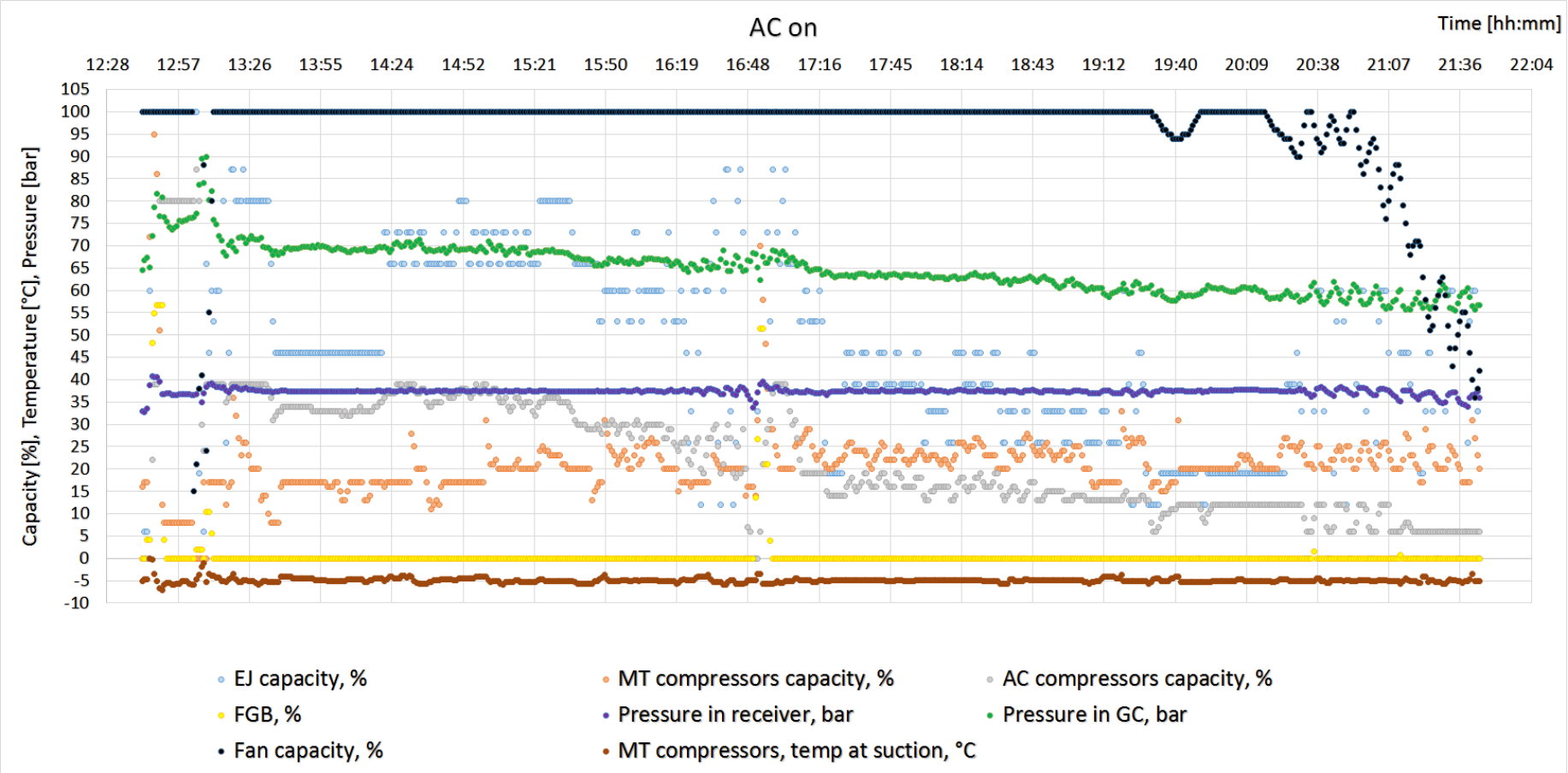

Figure 6.15 Refrigeration system in operation before the new ejector pack controller, AC on

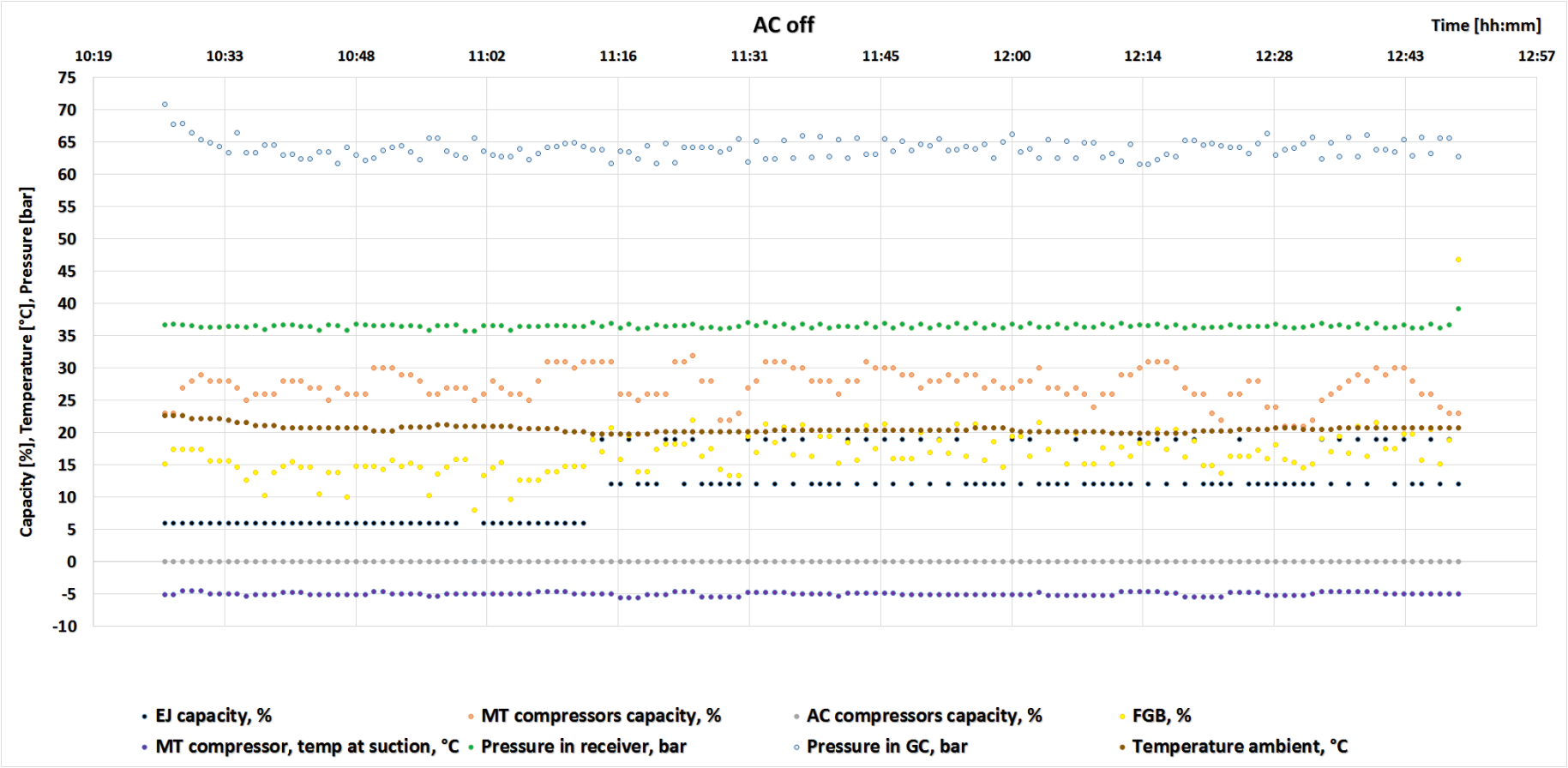

Figure 6.16 Refrigeration system in operation with the new ejector pack controller, AC off

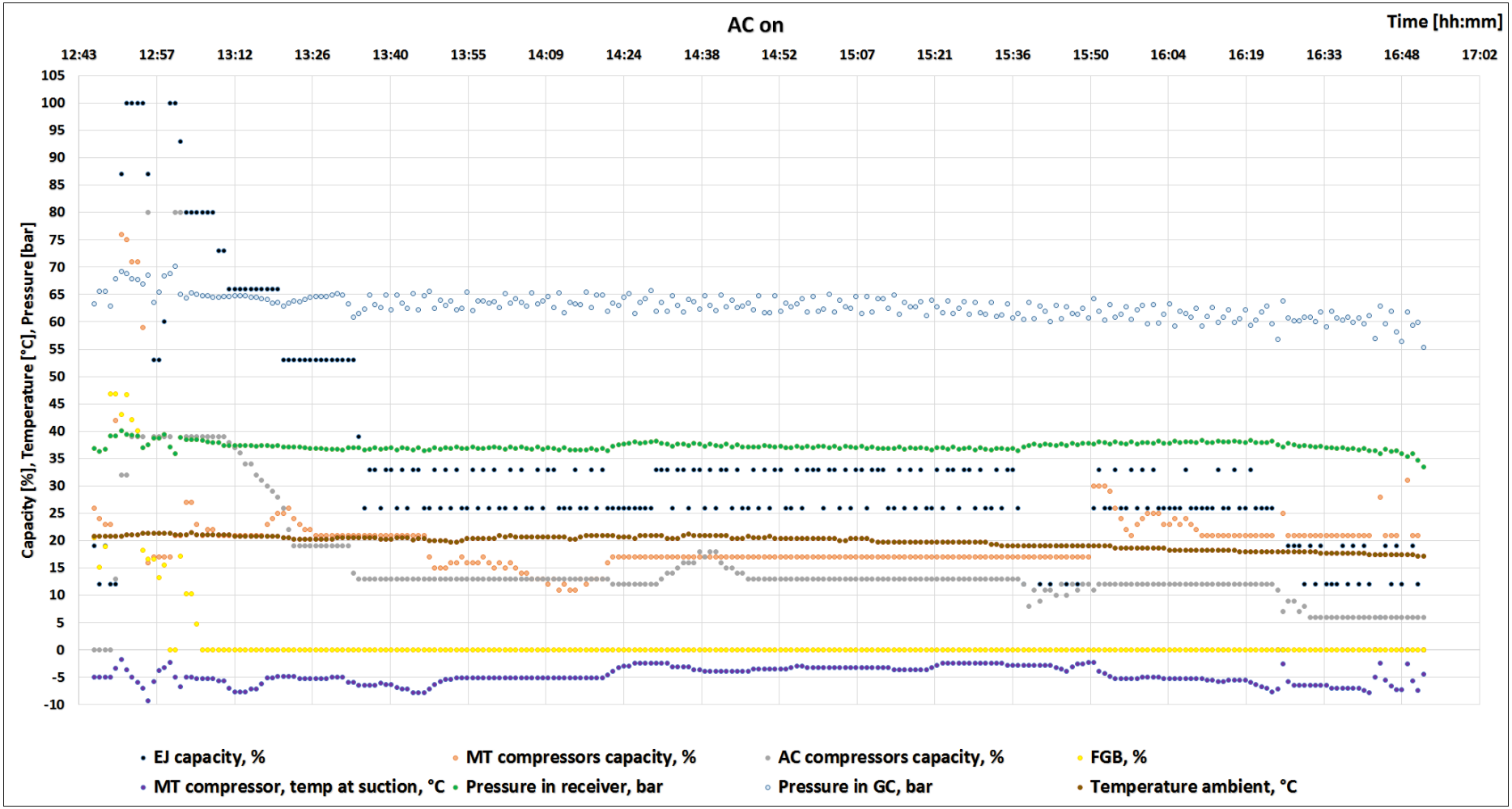

Figure 6.17 Refrigeration system in operation with the new ejector pack controller, AC on

In conclusion, on the basis of Fig. 6.14÷6.17 it can be noticed that:

- system used to work less stable before the installation of the new pack controller
- floating operation occurred especially when the AC was off (i.e. with a low load of the system), and this situation can be observed mainly in the performance of ejectors, fans and MT-compressors
- with the new pack controller system's work is much more steady, moreover, when the AC is on the operation is even more stable due to higher load of the system

7. CONCLUSIONS

The problem with oversized gas cooler, which caused unsteady system's operation, was handled by: switching the street-heating into permanently active mode, installation of a shut-off valve which reduces the gas cooler's capacity by 50% in case of low ambient temperature (< 7°C), reprogramming gas cooler's fans, and installation of a new pack controller for the ejectors. After this amendments, the system works more stable, especially during warmer days when the air conditioning is turned on. Other possible solution, which is impossible to implement in the system working in Rema 1000 Prinsensgata, is gas cooler's size reduction (by 50%) along with constraint in the number of fans. This means division of the gas cooler into two parts, with one part that constitutes 1/3 of the total length (with one fan), and the second one composed of 2/3 of the total length (with two fans). In this modification there is also an option of installing bypassing valve after the first part of the gas cooler, and air shutters which could restrain (cold) ambient air entering the gas cooler, thus avoiding a risk of low CO_2 outlet temperature. A simulation of the gas cooler operation was performed in a heat exchanger modelling computer program hXSIM (the Heat Exchanger Simulator), in order to achieve GC outlet temperature in an acceptable range for liquid separator's pressure level (i.e. not lower than 5°C) in view of the gas cooler split into two parts and increased subcooling with fairly stable GC outlet pressure (around 55 bar), hence more stable operation of the whole system and an increase in the COP is expected. The investigation depicted: maximal and minimal refrigerant flow rate that could be generated by MT-compressors, power demand for the MT-compressors and for the fans, and finally fans working range for different inlet air temperatures (within the scope of -15÷15°C) for two different inlet refrigerant temperatures (60°C and 20°C) and for boundary (maximal and minimal) refrigerant flow rates. A slightly subcooled liquid refrigerant was obtained after the first part with maximum air flow rate equal to 5.4 m^3/s, which is just enough to cope for two blowers (maximum air flow rate 5.66 m^3/s). In the second part of the GC maximal air flow rate, that was utilised, was not higher than 0.65 m^3/s, which is much below the maximum flow rate for one fan (i.e. 2.83 m^3/s).

8. PROPOSAL FOR FURTHER WORK

Other possible solutions that are still not implemented in Rema 1000 Prinsensgata, but would be beneficial for the system, are following:

- adapting the control of bypassing valve for the gas cooler and distributing heat towards the building and streets, which would prevent low gas cooler outlet temperature in the winter
- more frequent application of the AHU-heater, to heat up fresh air incoming to the supermarket when sufficient temperature has been reached inside the storage tanks (i.e. above 60°C), thus the GC load should diminish during the winter
- calibration of mass flow meter
- calibration of following energy meters: heat recovery, AC-evaporator, AHU-heater, snow-melting-unit
- varying temperature or pressure at the suction of MT-compressors to investigate energy savings

REFERENCES

ÇENGEL Y. A., BOLES M. A. 2011. Thermodynamics: an engineering approach. Seventh edition in SI units. New York: McGraw-Hill.

BOHDAL T., CHARUN H., CZAPP M. 2003. Urządzenia chłodnicze sprężarkowe parowe. Podstawy teoretyczne i obliczenia. Warszawa: Wydawnictwo Naukowo Techniczne.

GRZEBIELEC A., PLUTA Z., RUCIŃSKI A., RUSOWICZ A. 2011. Czynniki chłodnicze i nośniki energii.Warszawa: Oficyna Wydawnicza Politechniki Warszawskiej

DINÇER I., KANOĞLU M. 2010. Refrigeration systems and application. Second edition. John Wiley & Sons, Ltd.

FRELÉCHOX D. 2009. Field measurements and simulations of supermarkets with CO2 refrigeration systems (Master's thesis). KTH School of Industrial Engineering and Management. Division of Applied Thermodynamics and Refrigeration. Stockholm, Sweden.

MESSINEO A. 2012. R744-R717 Cascade Refrigeration System: Performance Evaluation compared with a HFC Two-Stage System. Energy Procedia, 14, 56-65.

GETU H. M., BANSAL P. K. 2008. Thermodynamic analysis of an R744–R717 cascade refrigeration system. International Journal of Refrigeration, 31, 45-54.

DA SILVA A., BANDARRA FILHO E. P. & ANTUNES A. H. P. 2012. Comparison of a R744 cascade refrigeration system with R404A and R22 conventional systems for supermarkets. Applied Thermal Engineering, 41, 30-35.

BANSAL P. 2012. A review – Status of CO2 as a low temperature refrigerant: Fundamentals and R&D opportunities. Applied Thermal Engineering, 41, 18-29.

GE Y. T. & TASSOU S. A. 2011. Thermodynamic analysis of transcritical CO2 booster refrigeration systems in supermarket. Energy Conversion and Management, 52, 1868-1875.

SAWALHA S., KARAMPOUR M., ROGSTAM J. 2015. Field measurements of supermarket refrigeration systems. Part I: Analysis of CO2 trans-critical refrigeration systems. Applied Thermal Engineering, 87, 633-647.

GIROTTO S., MINETTO S., NEKSA P. 2004. Commercial refrigeration system using CO2 as the refrigerant. International Journal of Refrigeration, 27, 717-723.

SHARMA V., FRICKE B., BANSAL P. 2014. Comparative analysis of various CO2 configurations in supermarket refrigeration systems. International Journal of Refrigeration-Revue Internationale Du Froid, 46, 86-99.

CHESI A., ESPOSITO F., FERRARA G., FERRARI L. 2014. Experimental analysis of R744 parallel compression cycle. Applied Energy, 135, 274-285.

SARKAR J. & AGRAWAL N. 2010. Performance optimization of transcritical CO2 cycle with parallel compression economization. International Journal of Thermal Sciences, 49, 838-843.

YAPICI R., ERSOY H. K. 2005. Performance characteristics of the ejector refrigeration system based on the constant area ejector flow model. Energy Conversion and Management, 46(18–19): 3117–35.

SARKAR J. 2009. Performance characteristics of natural-refrigerants-based ejector expansion refrigeration cycles. In: DEPARTMENT OF MECHANICAL ENGINEERING, I. O. T., BHU, VARANASI 221005, INDIA (ed.). Varanasi.

ELBEL S. & HRNJAK P. 2008. Experimental validation of a prototype ejector designed to reduce throttling losses encountered in transcritical R744 system operation. International Journal of Refrigeration-Revue Internationale Du Froid, 31, 411-422.

ELBEL S. 2011. Historical and present developments of ejector refrigeration systems with emphasis on transcritical carbon dioxide air-conditioning applications. International Journal of Refrigeration-Revue Internationale Du Froid, 34, 1545-1561.

SUMERU K., NASUTION H., ANI F. N. 2012. A review on two-phase ejector as an expansion device in vapor compression refrigeration cycle. Renewable & Sustainable Energy Reviews, 16, 4927-4937.

KORNHAUSER A. A. 1990. The Use of an Ejector as a Refrigerant Expander. International Refrigeration and Air Conditioning Conference. Purdue University: Purdue e-Pubs.

MENEGAY P. & KORNHAUSER A. A. 1996 Improvements to the ejector expansion refrigeration cycle. Energy Conversion Engineering Conference. IECEC 96., Proceedings of the 31st Intersociety, 11-16 Aug 1996 1996. 702-706 vol.2.

LI D. & GROLL E. A. 2005. Transcritical CO2 refrigeration cycle with ejector-expansion device. International Journal of Refrigeration, 28, 766-773.

DENG J. Q., JIANG P. X., LU T., LU W. 2007. Particular characteristics of transcritical CO2 refrigeration cycle with an ejector. Applied Thermal Engineering, 27, 381-388.

CHAIWONGSA P. & WONGWISES S. 2007. Effect of throat diameters of the ejector on the performance of the refrigeration cycle using a two-phase ejector as an expansion device. International Journal of Refrigeration, 30, 601-608.

HERDLITSCHKA T. 2016: Energy analysis of the ejector supported R744 vapour compression refrigeration systems at REMA 1000 Prinsensgate in Trondheim and Rif. POLI in Spiazzo Rendena, Department of Energy and Process Engineering, Norwegian University of Science and Technology.

HAFNER A. 2003: Compact Interior Heat Exchangers for CO¬2 Mobile Heat Pumping Systems, PhD Thesis, Faculty of Engineering Science and Technology, Department of Energy and Process Engineering, Norwegian University of Science and Technology.

PASTRICK T.W., ET AL. 2013: Active grill shutter vane design and vehicle system. US patent. Available at: google.com/patents/US20130223980.

APPENDIX A

HEAT EXCHANGER CALCULATION, USING HXSIM

```
H A H X  --  HXSIM v5.04-FEB-12-2007
Simulation
results                  ID: TEST CASE
Date: 17-APR-2016        Dataset: gascooler1
Time: 10:37

Status: Case did      converge after    5  iterationes

Type of heat exchanger: Gascooler

Tube concept: Tube-in-fin      Fin concept:  Plate
Tube variant: Round            Fin variant:  Plain
```

GEOMETRY:

MAIN DIMENSIONS:		TUBE BUNDLE AND LAMELLAS:	
Core length	: 6.340 m	Tube diameter(s)	: 8.50/7.30 mm H
Finned tube length	: 6.300 m		: 8.50/7.30 mm V
Core height	: 0.103 m	Fin thickness	: 0.12 mm
Core depth	: 1.122 m	Fin spacing	: 2.10 mm
Air side area	: 569.89 m	Fin material	:Aluminum
Tube inner area	: 25.67 m	Tube material	:Copper
Area ratio	: 22.41 -	Tube arrangement	
		: Staggered down	
		Number of vertical tubes:	2
Core weight	:249.714 kg	Vertical tube pitch:	41.00 mm
Tube weight	:150.078 kg	Number of horizontal tubes:	88
Fin weight	:99.636 kg	Horizontal tube pitch:	12.75 mm

OPERATING CONDITIONS:

Refrigerant side:

Inlet refrigerant temperature:	110.00 °C
Inlet refr. pressure:	90.00 Bar
Refrigerant flow:	0.8130 kg/s (2926.8 kg/h)
Refrigerant:	CO_2

Air side:

Inlet air temperature	: 30.00 °C
Relative humidity	: 60.00 %
Air face velocity	: 1.20 m/s
Air flow	: 8.490 m^3/s (30564 m^3/h)
Air flow (standard)	: 7.880 Sm^3/s (28370 Sm^3/h)
Air flow direction	: South

HEAT PERFORMANCE CALCULATION SUMMARY:

Main results

Performance	:	184.21 kW
Overall heat transfer coefficient	:	30.44 W/m˛°C
Exit temperature difference	:	4.97 K

Air side:

Mean heat flux	:	323.25 W/m
Pressure drop	:	26.66 Pa
Theoretical fan power demand	:	226.30 W

Refrigerant side :

Mean heat flux	:	7175.33 W/m
Pressure drop (including headers)	:	18.94 kPa (0 K)
(Without headers)	:	19.37 kPa
Total refrigerant flow	:	0.8130 kg/s (48.78 kg/min)
Refrigerant content	:	20929.26 g
Refrigerant content, liquid only	:	31720.50 g
Outlet temperature	:	34.97 °C
Outlet vapour quality (average)	:	1.00 -

GEOMETRY CALCULATIONS:

MAIN DIMENSIONS:

Core length :	6.340 m	Air side area	: 569.89 m
Finned tube length:	6.300 m	Tube inner area	: 25.67 m
Core height :	0.103 m	Area ratio	: 22.41 -
Core depth :	1.122 m	Air face area	: 7.069 m

Core weight	: 249.714 kg	Fin area	: 541.89 m
Tube weight	: 150.078 kg	Air side	
Fin weight	: 99.636 kg	tube area	: 28.00 m
		Contraction ratio	: 0.95 -

TUBE BUNDLE AND FIN DATA:

Tube Data

Tube variant	:	Round
Tube diameter	:	8.50/7.30mm
Return bend diameter	:	23.80/25.00mm
Tube wall thickness	:	0.60 mm
Tube enhancement factors,		
- Refrigerant side heat transfer	:	1.00
- Corresponding pressure drop increase	:	1.00
- Refrigerant side surface	:	1.00
- Air side heat transfer	:	1.00
- Corresponding pressure drop increase	:	1.00
- Air side surface	:	1.00
Tube material,	:	Copper
- Thermal conductivity	:	400.00 W/m K
- Density	:	8950.00 kg/m^3
Tube weight,		
- Total weight	:	150.08 kg
- Weigth per meter	:	0.1333 kg/m

Fin data

Fin variant	:	Plain
Fin thickness	:	0.12 mm
Fin spacing	:	2.10 mm
Total number of fins	:	3000 -
Fixed fin efficiency	:	**0.86 %**
Fin enhancement factors		
- Heat transfer enhancment	:	**1.17 -**
- Corresponding pressure drop increase	:	1.16 -
Fin material,	:	Aluminum
- Thermal conductivity	:	230.00 W/m K
- Density	:	2750.00 kg/m^3

APPENDIX B

Table 2 Refrigerant flow for the MT-compressors, range of work 22÷42%

Scope of work, %	Frequency, Hz	Displacement, $\frac{m^3}{h}$	Mass flow, $\frac{kg}{s}$
22	30	6.97	0.121
23	31.5	7.32	0.127
24	33	7.67	0.133
25	34.5	8.02	0.139
26	36	8.37	0.145
27	37.5	8.722	0.151
28	39	9.06	0.157
29	40.5	9.41	0.163
30	42	9.76	0.169
31	43.5	10.11	0.175
32	45	10.46	0.181
33	46.5	10.81	0.187
34	48	11.16	0.194
35	49.5	11.50	0.200
36	51	11.85	0.206
37	52.5	12.20	0.212
38	54	12.55	0.218
39	55.5	12.90	0.224
40	57	13.25	0.230
41	58.5	13.60	0.236
42	60	13.94	0.242

Table 3 Refrigerant flow for the MT-compressors, range of work 28÷50%

Scope of work, %	Frequency, Hz	Displacement, $\frac{m^3}{h}$	Mass flow, $\frac{kg}{s}$
28	30	9.82	0.170
29	31.4	10.26	0.178
30	32.7	10.71	0.186
31	34.1	11.15	0.193
32	35.5	11.60	0.201
33	36.8	12.05	0.209
34	38.2	12.49	0.217
35	39.5	12.94	0.224
36	40.9	13.39	0.232
37	42.3	13.83	0.240
38	43.6	14.28	0.248
39	45	14.72	0.255
40	46.4	15.17	0.263
41	47.7	15.62	0.271
42	49.1	16.06	0.279
43	50.5	16.51	0.286
44	51.8	16.95	0.294
45	53.2	17.40	0.302
46	54.5	17.85	0.310
47	55.9	18.29	0.317
48	57.3	18.74	0.325
49	58.6	19.19	0.333
50	60	19.63	0.341